Cre-Controlled CRISPR (3C) Mutagenesis: Fast and Easy Conditional Gene Inactivation in Zebrafish

Stefan Hans (stefan.hans@tu-dresden.de)
Technische Universität Dresden https://orcid.org/0000-0003-0283-0211

Daniela Zöller
Technische Universität Dresden

Juliane Hammer
Technische Universität Dresden

Johanna Stucke
Technische Universität Dresden

Sandra Spieß
Technische Universität Dresden

Gokul Kesavan
Center for Regenerative Therapies Dresden, Center for Molecular and Cellular Bioengineering

Volker Kroehne
Technische Universität Dresden

Juan Sebastian Eguiguren
Technische Universität Dresden https://orcid.org/0000-0002-8866-4316

Diana Ezhkova
Technische Universität Dresden

Andreas Petzold
Dresden University of Technology

Andreas Dahl
Technische Universität Dresden https://orcid.org/0000-0002-2668-8371

Michael Brand
Centre for Regenerative Therapies, Dresden

Research Article

Keywords: conditional gene inactivation, Cre/lox, CRISPR/Cas9, pigmentation, zebrafish

Posted Date: September 16th, 2020

DOI: https://doi.org/10.21203/rs.3.rs-72885/v1

Version of Record: A version of this preprint was published at Nature Communications on February 18th, 2021. See the published version at https://doi.org/10.1038/s41467-021-21427-6.

Cre-Controlled CRISPR (3C) mutagenesis: fast and easy conditional gene inactivation in zebrafish

Stefan Hans*[1], Daniela Zöller[1], Juliane Hammer[1], Johanna Stucke[1], Sandra Spieß[1], Gokul Kesavan[1], Volker Kroehne[1], Juan Sebastian Eguiguren[1], Diana Ezhkova[1], Andreas Petzold[2], Andreas Dahl[2] and Michael Brand*[1]

[1] Technische Universität Dresden, Center for Molecular and Cellular Bioengineering (CMCB), CRTD - Center for Regenerative Therapies Dresden, Fetscherstraße 105, 01307 Dresden, Germany

[2] Technische Universität Dresden, Center for Molecular and Cellular Bioengineering (CMCB), DRESDEN-Concept Genome Center, Fetscherstraße 105, 01307 Dresden, Germany

* Corresponding authors

Running title: Conditional gene inactivation using CRISPR

Key words: conditional gene inactivation; Cre/lox; CRISPR/Cas9; pigmentation; zebrafish

Abstract

Conditional gene inactivation is a powerful tool to determine gene function when constitutive mutations result in detrimental effects. The most commonly used technique to achieve conditional gene inactivation employs the Cre/loxP system and its ability to delete DNA sequences flanked by two loxP sites. However, targeting critical exons or an entire gene with two loxP sites is time and labor consuming. To circumvent these issues, we developed Cre-Controlled CRISPR (3C) mutagenesis. 3C mutagenesis is simple, fast and allows gene inactivation in a Cre-dependent manner. In contrast to loxP-flanked alleles, the recombined cells become fluorescently visible enabling the isolation of these cells and their subjection to various omics techniques. Moreover, 3C will be scalable and will enable the conditional inactivation of multiple genes simultaneously. Hence, 3C mutagenesis provides a valuable alternative to the production of loxP-flanked alleles and should be applicable to all model organisms amenable to single integration transgenesis.

Introduction

Gene inactivation is the most powerful tool to determine gene function. Forward genetic screens in yeast, *C. elegans*, and *Drosophila* produced numerous mutants revealing genes and pathways controlling cell biology and development (Botstein and Fink, 1988; Brenner, 1974; Nüsslein-Volhard and Wieschaus, 1980). Similarly, saturation mutagenesis of the zebrafish genome yielded an array of mutations affecting all aspects of vertebrate development (Nüsslein-Volhard, 2012). In mammalian species, reverse genetics is the dominant approach, building on precise gene targeting via homologous recombination in embryonic stem cells which has revolutionized the study of mammalian biology and human medicine (Capecchi, 2005). Nowadays, designer nucleases like Zinc-finger nucleases (ZFNs), transcription activator-like effector nucleases (TALENs) and in particular clustered regulatory interspaced short palindromic repeat (CRISPR)/Cas9 are used for a broad range of tailor-made genomic modifications in almost all model organisms (Gaj et al., 2013). Designer nucleases enable targeted DNA double strand breaks that stimulate repair mechanisms which can subsequently be exploited for the generation of knock-out and knock-in alleles (Cubbon et al., 2018). Knock-outs are achieved by error-prone non-homologous end joining DNA repair introducing small frameshift insertion-deletions (indels) in the coding sequence and the usage of resulting premature stop codons (Jao et al., 2013). Knock-in generation employs either homology-directed repair for the precise integrations of small sized cargo or homology-independent double strand break repair for the insertion of larger DNA cassettes (Auer et al., 2013; Bedell et al., 2012; Shin et al., 2014).

Although mutations are key to understand gene function, the above-mentioned constitutive gene inactivations often result in detrimental effects including embryonic lethality, due to its consequences for all cells. Consequently, the analysis of gene function at later stages is impeded or impossible. To solve this issue, conditional gene inactivation strategies have been developed. In organisms with efficient forward genetics, temperature-sensitive alleles have been generated (Hirsh and Vanderslice, 1976; Suzuki, 1970). Temperature-sensitive mutations are typically missense mutations, which retain protein function at permissive temperatures but fail to work properly at restrictive temperatures. In mammals, the most commonly used technique to achieve conditional gene inactivation employs the Cre/loxP system (Yarmolinsky and Hoess, 2015). Cre recombinase promotes strand exchanges between two loxP target sites and depending on their orientation, recombination results either in the excision or inversion of the intervening DNA sequence. Thus, conditional gene inactivation can be achieved in a Cre-dependent manner if a gene or critical exon is flanked by loxP sites (floxed). Ligand-inducible Cre variants ($CreER^{T2}$) offer additional temporal control of Cre-mediated recombination and allow targeting later aspects of a dynamic Cre expression (Feil, 2007). CRISPR/Cas9 technology now also allows targeting loci with two loxP sites in other species like zebrafish (Burg et al., 2018; Hoshijima et al., 2016). However, establishment of a floxed allele and the generation of animals carrying the desired genetic composition is time and labor consuming. Moreover, although dual fluorescent gene-labeling has been reported recently (Li et al., 2019), floxed alleles are usually unlabeled impeding an easy recognition of mutant cells. Finally, Cre-mediated gene inactivation of floxed alleles requires

two independent recombination events which is difficult to achieve in tissues with low recombination efficiencies (Becher et al., 2018). Hence, we devised an alternative approach developing Cre-Controlled CRISPR (3C) mutagenesis as an easy and straightforward system that allows conditional gene inactivation in a Cre-dependent manner. 3C mutagenesis relies on a Cre effector construct with a promoter driving a floxed first open reading frame like a Stop cassette upstream of a second open reading frame encoding a Cas9-GFP fusion protein (Fig. 1A). The same transgenic construct expresses a gRNA targeting a gene of interest (GOI) under the zebrafish *U6a* promoter. In the default, unrecombined condition only the gRNA but no Cas9-GFP is present. Consequently, no functional Cas9/gRNA ribonucleoprotein complex is formed and the gene of interest remains intact. In contrast, an active Cas9/gRNA ribonucleoprotein complex is present in the cells after a successful Cre-mediated recombination event resulting in mutagenesis of the gene of interest. After using this approach transiently to conditionally inactivate *cdh2* in the anterior neural plate in a Cre-dependent manner (Kesavan et al., 2020), we show here the functionality with stable transgenic lines. As a proof-of-principle, we used a well-established target site in *tyrosinase*, the gene encoding the enzyme required for converting tyrosine into the pigment melanin. We demonstrate the functionality of 3C mutagenesis using Cre mRNA injections and various Cre/CreER^{T2} driver lines, resulting in pigmentation loss in a Cre-dependent manner. Single-end next generation sequencing confirmed high level mutagenesis in recombined cells. Taken together, our 3C conditional gene inactivation system is simple, fast and allows gene inactivation in a Cre-dependent manner. Moreover, 3C mutagenesis is scalable and will enable the conditional inactivation of multiple genes simultaneously. Finally, following Cre-mediated recombination and expression of Cas9-GFP, presumptive mutant cells become fluorescently visible which enables the isolation of these cells and their subjection to various downstream omics techniques, like transcriptomics. Hence, 3C mutagenesis provides a valuable alternative to the production of floxed alleles and has the potential for applications in other model organisms amenable to single integration transgenesis.

Results

Establishment of a 3C gene inactivating line targeting tyrosinase

In order to test the rationale of Cre-Controlled CRISPR (3C), we generated a Tol2 transposon-based vector comprising the temperature-inducible *heat shock cognate 70-kd protein, like* (*hsp70l*) promoter controlling expression of a floxed DsRed cassette upstream of the coding sequence of a Cas9-GFP fusion protein (Fig. 1B). In addition, the vector contained a zebrafish *U6* promoter (*U6a*) to drive transcription of a gRNA targeting *tyrosinase* (*tyr*) (Jao et al., 2013; Yin et al., 2015). We chose to target *tyr* because it encodes the enzyme converting tyrosine into the pigment melanin. In zebrafish, *tyr* is expressed in cells of the retinal pigment epithelium (RPE) and in neural crest-derived melanocytes from 16.5 and 18 hours post fertilization (hpf), respectively (Camp and Lardelli, 2001). Consequently, mutagenesis of *tyr* prior to gene onset results in pigmentation defects in the developing eye and body, offering an easy read-out of biallelic gene inactivation (Jao et al., 2013). Using Tol2 transposon-mediated transgenesis (Kawakami, 2004), we identified eleven founders out of twenty-one animals screened using DsRed as a transgenesis marker present at 48 hpf after a 30 minute heat treatment at 24 hpf (Fig. 1C). Four founders were used to establish stable transgenic lines (referred as 3C *tyr* henceforward).

Cre mRNA injection results in ubiquitous GFP expression and widespread pigmentation loss

Adult 3C *tyr* animals were crossed to wild-type and the resulting progeny were injected with *in vitro* transcribed Cre mRNA at the 1-cell stage, eliciting recombination during early stages of development (Fig. 2A). Following a heat treatment at 12 hpf, which activates Cas9-GFP-mediated mutagenesis in recombined cells, animals were analyzed at 22 and 50 hpf to score GFP expression and pigmentation, respectively. In comparison to uninjected controls, we observed a broad, ubiquitous GFP fluorescence in Cre mRNA injected animals at 22 hpf (Fig. 2B). At 50 hpf, GFP-positive embryos displayed a strong pigmentation loss within the developing eye and body (Fig. 2C, D). Importantly, all animals showing GFP expression also displayed pigmentation defects if the heat treatment was applied prior to onset of *tyr* expression. Animals heat treated later but still prior to first signs of pigmentation (22 hpf), also showed strong GFP expression but displayed a normal pigmentation pattern (data not shown). To quantify the mutation rate, we repeated the above mentioned experiment to obtain GFP-positive cells from 30 Cre mRNA injected embryos and control cells from 30 siblings, respectively (Suppl. Fig. 1A). In order to ensure the analysis of the *tyr* locus from cells only with successful Cas9-GFP expression, we employed fluorescence-activated cell sorting (FACS) at 24 hpf which showed the presence of GFP-negative cells also in Cre mRNA injected embryos (Suppl. Fig. 1B). Following genomic DNA extraction from the FAC-sorted cells, the DNA was used as a template for a locus-specific PCR amplifying the region targeted by the *tyr* gRNA. Subsequently, the amplified PCR fragments were used in single-end next generation sequencing and the genome editing was analyzed using CRISPResso2 (Clement et al., 2019). In control cells, we found a single nucleotide polymorphism (SNP) in the first

position of the protospacer adjacent Motif *(*PAM). However, because any nucleotide is accepted in the canonical Cas9 PAM sequence NGG, this finding has no negative consequences with respect to targeting efficacy and only results in the presence of two parental sequences (Fig. 3A). In control cells, the parental strands can be detected with a proportion of 48.26% and 38.46%, respectively (Fig. 3B). In sharp contrast, the proportion of parental strands drops to 7.15% and 0.48% in GFP-positive cells and variable indels are abundantly present (Fig. 3C, Suppl. Fig. 2). We also analyzed off-target effects in the control and GFP-positive cells. The web tool for CRISPR- and TALEN-based genome editing CHOPCHOP (Labun et al., 2019) identifies one potential off-target on chromosome 19 with three mismatches to our employed *tyr* gRNA (Suppl. Fig. 3A). However, locus-specific amplification, single-end sequencing and CRISPResso2 analysis reveals highly similar allele frequencies with 83.1% in control and 88.55% in GFP-positive cells (Suppl. Fig. 3B). Taken together, these data show that our 3C *tyr* gene inactivation line robustly mediates biallelic gene disruptions in the RPE and in neural crest-derived melanocytes with no further side effects.

Spatially-controlled Cre activity results in tissue-specific GFP expression and restricted pigmentation loss

To test gene inactivation in a tissue-specific manner, we combined our 3C *tyr* lines with Cre driver lines which allowed us to interfere independently with *tyr* activity in either RPE cells or in neural crest-derived melanocytes. To achieve the former, we made use of a knock-in of the inducible variant of Cre ($CreER^{T2}$) into the endogenous *otx2b* locus (Kesavan et al., 2018). For the latter, we used a transgenic line expressing Cre under a fragment of the zebrafish *sox10* promoter (Rodrigues et al., 2012). In *sox10*:Cre, Cre expression is initiated at 10 hpf resulting in Cre-mediated recombination in cells of the developing neural crest (Fig. 4A). Following a heat treatment at 16 hpf, we observed GFP fluorescence in neural crest cells at 22 hpf (Fig. 4B). At 50 hpf, neural-crest derived body pigmentation is present in control animals with no striking difference in GFP-positive embryos (Fig. 4C). However, closer examination revealed a reduction of pigmentation in the head region (Fig. 4D). This finding was further corroborated when GFP-positive animals were raised to adulthood. At this stage, mutant cells cover larger surface areas and displayed a loss of pigmentation in two vertical stripes as well as in the pectoral fins (Suppl. Fig. 4A). Because *sox10* expression is not initiated in all neural crest cells simultaneously, but in an anterior to posterior wave (Suppl. Fig. 4B), we hypothesized that the selected six hour time window, in which Cre-mediated recombination and heat treatment-induced mutagenesis are happening, is too tight and hence causative for the mild observed pigmentation phenotype. To test this hypothesis, we repeated the experiment but provided three consecutive heat treatments at 16, 22 and 28 hpf to elicit gene inactivation in more cells (Suppl. Fig. 4C). Indeed, a further reduction in body pigmentation was observed (Suppl. Fig. 4D). Importantly, pigmentation in the RPE cells of the developing eyes was never affected in GFP-positive embryos neither in single nor triple heat treated animals. To achieve tissue-specific gene inactivation in RPE cells, we used *otx2b:*$CreER^{T2}$ in which a knock-in of the $CreER^{T2}$ coding sequence recapitulates the endogenous *otx2b*

expression (Kesavan et al., 2018). *otx2b* is initiated at 6 hpf and expressed in cells of the anterior neural plate including the eye field throughout early development. In order to induce widespread recombination, we applied 4-Hydroxytamoxifen (4OHT) at the onset of *otx2b* expression (Fig. 5A). Following a heat treatment at 12 hpf, strong GFP expression is observed in the anterior brain including the developing eyes, fore- and midbrain at 22 hpf (Fig. 5B). At 50 hpf, body pigmentation is indistinguishable in control and GFP-positive embryos (Fig. 5C). However, we observe a strikingly significant reduction of pigmented cells in the developing eye in GFP-positive embryos in comparison to controls (Fig. 5D). Importantly, GFP fluorescence and pigmentation defects were only displayed after application of both, 4OHT and a heat treatment, but never elicited in the presence of 4OHT or heat treatment only. In summary, these data show that our 3C *tyr* lines can be used for tissue-specific biallelic gene inactivation in a conditional Cre-dependent manner.

A recombined 3C *tyr* transgene allows temporally-controlled gene inactivation and is transmitted to the next generation

The above mentioned experiments show that 3C gene inactivation can be used simply as a regular Cre effector line which, in combination with a Cre driver, allows spatiotemporally-controlled mutagenesis of a gene of interest. However, because the number of available Cre driver lines is still limited in zebrafish, and moreover, experimental designs might require loss-of-function in the entire organism, we addressed ubiquitous, temporally-controlled only gene inactivation. To do so, we made use of the conditional nature of the *hsp70l* promoter which is only active after a heat treatment but not at permissive temperatures (Halloran et al., 2000). Hence, it should be possible to decouple recombination and mutagenesis if Cre activity but no heat treatment is applied. However, a basal leakiness has been reported for the *hsp70l* promoter (Hans et al., 2011) which might result in non-conditional mutagenesis of the target gene. To test this, we repeated the above mentioned Cre mRNA injection experiment to elicit recombination at early stages in an almost ubiquitous fashion (Fig. 4A). One subset of injected embryos was heat treated at 12 hpf, a second at 60 hpf and successful recombination was identified via GFP expression at 24 or 72 hpf, respectively. A third subset that never underwent a heat treatment was collected at 120 hpf. Because Cre mRNA injected 3C *tyr* transgenic animals are indistinguishable from wild-type siblings in the absence of a heat treatment, we established a 3C-specific PCR which even allowed the identification of recombined and non-recombined alleles (Suppl. Fig. 5A, B). This PCR strategy was applied to single embryos of all three time points (heat: none; heat: 12 hpf; heat 60 hpf) as well as various controls (wild-type, 3C *tyr*; no Cre, no heat treatment, 3C *tyr*; no Cre, with heat treatment) to verify the genotype of each embryo (Suppl. Fig. 5C). Subsequently, the genomic DNA of ten embryos per sample were combined and analyzed using single-end next generation sequencing (NGS). Finally, GFP-positive siblings identified at 12 hpf and 60 hpf as well as siblings never subjected to a heat treatment were raised to adulthood. Importantly, Cre mRNA injected animals, which were never subjected to a heat treatment, were indistinguishable from controls at embryonic and adult stages (Fig. 6B, Suppl. Fig. 6C, D). Also, sequencing of the *tyr* locus in the 120 hpf animals, which were exposed to Cre but no heat, confirmed an unmodified locus with a

proportion of the parental strands at 76.80% and 14.10%. Genotyping of adult animals confirmed recombined 3C *tyr* alleles indicating its inactivity during growth. In sharp contrast, animals heat treated at 12 hpf, displayed a strong pigmentation phenotype at 50 hpf which persisted well into adulthood (Fig. 6C). Consistent with strong pigmentation defects observed at embryonic stages, the loss of pigmentation was also present in adult animals, although variable amounts of pigmented cells could be detected (Fig. 6C, Suppl. Fig. 6A). High level mutagenesis was confirmed by NGS when variable indels were abundantly present and the proportion of the parental strands dropped to 20.64% and 0.85% (Fig. 6C, Suppl. Fig. 6E). The proportion of parental strands in control samples (wild-type, 3C *tyr*; no Cre, no heat treatment, 3C *tyr*; no Cre, with heat treatment) was always >90% (Suppl. Fig. 6F). Animals heat treated at 60 hpf displayed naturally the normal pigmentation pattern at 50 hpf, identical to controls (Fig. 6D). However, variable pigmentation loss was evident at adult stages (Fig. 6D, Suppl. Fig. 6B). Mutagenesis of the *tyr* target site was also confirmed via sequencing with the parental strands present with only 67.62% and 16.02%. To test if the recombined 3C *tyr* locus is successfully transmitted and can be reactivated again, we crossed animals exposed to Cre activity but no heat treatment with wild-type. Subsequently, progeny underwent a heat treatment at 12 hpf. Indeed, following a strong and ubiquitous GFP expression at 22 hpf, we observe a strong reduction in pigmentation of the body and developing eye (Fig. 6E). Taken together, these results show that Cre-mediated recombination and Cas9-mediated gene inactivation can be decoupled and that the basal leakiness of the *hsp70l* promoter does not increase non-conditional mutagenesis. Moreover, the recombined 3C *tyr* locus is stably inherited and can be reactivated to mutagenize the target gene.

Discussion

Previous reports showed that transgenic zebrafish with stable Cas9 and gRNA expression can be used to induce biallelic gene inactivation in somatic cells (Ablain et al., 2015; Yin et al., 2015). However, these approaches remained either non-conditional because Cas9 activity was only spatially controlled in a single transgene or genetically challenging because it required the presence of three different transgenes providing expression of a gRNA, a Cre-controlled Cas9 and Cre activity. Moreover, in neither of these cases Cas9 expressing and hence putative mutant cells were labelled. Here, we now introduce Cre-Controlled CRISPR or 3C mutagenesis to achieve conditional gene inactivation building on the binary Cre/loxP system. Binary systems offer the advantage that driver and effector lines are initially established independently and without any detrimental effects. In this context, a 3C gene inactivation line can be generated like any other Cre effector line which is easily achieved in many organisms, including zebrafish, via Tol2 transposon-mediated transgenesis (Kawakami, 2004). Following transposon-mediated transgenesis, the 3C gene inactivation line requires Cre activity to delete the floxed first open reading frame and to allow Cas9-GFP expression. In combination with the ubiquitously present gRNA, also driven from the same effector construct, a functional Cas9/gRNA ribonucleoprotein complex is formed triggering mutagenesis of the target site. In the best scenario, Cre activity is provided via a Cre driver line which allows precise spatial-temporal resolution *in vivo* as we showed with biallelic gene inactivation of *tyrosinase* in neural crest-derived melanocytes by using a *sox10*:Cre expressing transgene and in the developing eye by using an *otx2b*:CreER^{T2} expressing transgene. However, also exogenously delivered Cre activity is possible. Potential approaches might include *in vivo* electroporation of Cre expressing plasmids or Cre transgene delivery via herpes simplex type I viruses into different organs at various developmental and adult stages (Cerda et al., 2006; Zou et al., 2014). We used Cre mRNA injections at the 1-cell stage to elicit recombination at the earliest time point possible which resulted in pigmentation defects in both neural crest-derived melanocytes and anterior neural plate-derived RPE cells. However, our phenotypic as well as sequence analysis show that mutations can also be induced in a temporally-controlled manner. At 50 hpf, Cre mRNA injected embryos displayed a normal pigmentation pattern and were indistinguishable from wild-type controls. Following a heat treatment at 60 hpf, indels were present in animals analyzed twelve hours later and moreover, siblings raised to adulthood displayed various pigmentation defects. When compared to embryos heat treated at 12 hpf, the mutagenesis rate in embryos heat treated at 60 hpf was significantly reduced. However, this only indicates that the heat treatment applied at 12 hpf is not sufficient to induce indels in the same manner at 60 hpf. Hence, higher mutagenesis rates require adjustments to the heat treatment regime which we have shown previously can also be applied at adulthood (Kroehne et al., 2011). Alternatively to Cre mRNA injections, also a Cre driver can be used for tissue-specific recombination at early stages followed by heat treatment to activate the *hsp70l* promoter at later stages to elicit mutagenesis. This way also some spatial control can be provided and mutagenesis is restricted to a certain lineage. Cre mRNA injections at the 1-cell stage can also be used to generate F1 animals carrying the recombined 3C gene inactivation construct in all cells. In our experiments, FACS revealed the presence of GFP-negative cells also in Cre mRNA injected embryos indicating that not all cells

undergo recombination upon Cre mRNA delivery. Consequently, mutagenesis of the *tyr* target site also does not occur in non-recombined cells. This notion is supported by our sequencing data which show that the proportion of the parental strands in GFP-positive cells enriched via FACS increases from 7.63% (7.15% + 0.48%, Fig. 1) to 21.49% (20.64% + 0.85%, Fig. 6) in cells obtained from GFP-positive embryos without FACS enrichment. However, because recombined cells also contribute to the germline, the recombined 3C gene inactivation construct is transmitted to the next generation. Here it can be activated in a temporally-controlled manner and, due to its presence in all cells, should theoretically result in a higher proportion of mutated target sites. In our proof-of-principle, we did not observe any obvious differences in pigmentation defects when comparing heat treated F0 animals subjected to Cre mRNA injection and heat treated F1 animals carrying a recombined 3C *tyr* allele. However, because the selected *tyr* target site has been shown to be highly efficient (Jao et al., 2013), the potential increase might be hidden in the variable pigmentation phenotypes obtained. Nevertheless, the approach to generate animals carrying a recombined 3C allele in all cells might be reasonable for 3C gene inactivation lines driving less efficient gRNAs to mutate other targets.

Compared to the production of floxed alleles, our 3C gene inactivation offers several advantages. First, 3C mutagenesis is fast because preliminary loss-of-function analysis can already take place in the F1 generation when the 3C founder (F0) possesses a good transmission rate and is subsequently crossed to a Cre driver to obtain progeny carrying both transgenes. In contrast, time consuming locus-specific genetic engineering is required for the generation of a floxed allele. Introduction of loxP sites flanking the entire locus or a critical exon is executed either sequentially or simultaneously in zebrafish (Burg et al., 2018; Hoshijima et al., 2016). However, even if the floxed locus is achieved with one round of genetic engineering, the subsequent breeding to obtain animals carrying the floxed locus in homozygosity and a Cre driver allele takes at least two generations. Second, putative mutant cells are genetically labelled due to the expression of Cas9-GFP. This will allow the implementation of lineage tracing studies of putative mutant cells in an otherwise wild-type context. Moreover, fluorescently labelled and putative mutant cells can be easily isolated using fluorescence-activated cell sorting (FACS). Their subsequent subjection to various omics techniques (e.g. transcriptomics) will provide additional details of cellular events in the absence of the gene of interest. In contrast, the mutant or wild-type status of floxed alleles is usually not provided via a fluorescent readout impeding an easy recognition of mutant cells. Only recently, a dual fluorescent gene-labeling strategy has been reported, which however, still requires locus-specific genetic engineering (Li et al., 2019). Third, 3C gene inactivation is scalable and will hence enable the conditional inactivation of multiple genes simultaneously. In our proof-of-principle study, we used a single gRNA driven by the zebrafish *U6a* promoter to target the open reading frame in the first exon of *tyrosinase*. A single gRNA was used because the target site has already been shown to be highly efficient (Jao et al., 2013). For future 3C gene inactivation lines, it is recommended to employ two gRNAs because two guides are more effective in disrupting gene function than a single gRNA due to induction of small genomic deletions, in addition to frameshifts caused by indel mutations (Wu et al., 2018). Expression of a second, third and fourth gRNA is achieved using additional *U6* promoters

which have been analyzed for this purpose (Yin et al., 2015) and which can be easily added into our 3C gene inactivation construct. Because the targeting efficiency of the guides is the most critical aspect in 3C gene inactivation, several guides should be tested transiently as recently described (Shah et al., 2015). Subsequently, the two most efficient guides should be selected for the generation of the 3C gene inactivation construct employed in Tol2 transposon-mediated transgenesis. In contrast to potential inactivation of multiple genes via 3C, conditional gene inactivation with two or even more floxed alleles is theoretically feasible. However, generation of the floxed loci and subsequent breeding to obtain the desired genetic composition is very time consuming. Moreover, unintentional inter-chromosomal recombination can cause unwanted, detrimental side effects. Finally, a single recombination event allows for the expression of Cas9-GFP in our 3C gene inactivation system which is beneficial in tissues with low recombination efficiencies. Using Cre/loxP-based genetic lineage-tracing, we previously showed that *her4.3*-positive ventricular radial glia cells react to injury and generate new neurons in the zebrafish telencephalon (Kroehne et al., 2011). Despite broad expression of $CreER^{T2}$ in a large proportion of the ventricular zone, we observed only limited recombination, most likely due to low local concentrations of 4-Hydroxytamoxifen. Although, low recombination will persist also with 3C, the number of putative mutant cells will be identical to the number of cells observed in the genetic lineage tracing experiment and we will be able to follow their fate in a wild-type context due to Cas9-GFP expression. In contrast, Cre-mediated gene inactivation of floxed alleles requires two independent recombination events to elicit the mutant situation. Consequently, the number of mutant cells would be significantly further reduced in our tissue of interest. In conjunction with the absence of a genetic label it will be almost impracticable to recognize mutant cells.

Our newly developed Cre-Controlled CRISPR (3C) will allow conditional gene inactivation studies and represents a valuable alternative to the production of floxed alleles requiring only the generation of one transgenic line. However, Tol2 transposon-mediated transgenesis usually results in the integration of multiple copies of transgenes at random loci within the genome (Kawakami, 2004). Subsequently, time consuming characterization is required to identify integrations displaying the desired properties like expression level and pattern. Targeted, site-directed transgene integration into pre-determined genomic loci can circumvent these issues. The integrase PhiC31 catalyzes an unidirectional recombination between heterotypic *attP* and *attB* sites and its functionality has already been shown in zebrafish (Mosimann et al., 2013). In the long run, it will be beneficial to establish an *attP* landing site line in a safe harbor locus for 3C-mediated gene inactivation. 3C is a composite of a generic Cre effector construct that switches to Cas9-GFP after a successful recombination event and a U6 promoter cassette expressing a gRNA for gene-specific mutagenesis. Integration of the *attP* sequence into the generic 3C effector construct will result in a general platform for future 3C gene inactivation lines. The 3C landing site line needs to undergo thorough characterization only during its establishment. Subsequently, the *attP*/*attB*-mediated integrations can be directly used in a planned experimental setup because no further negative positional effects are expected. We foresee that the generation of a 3C landing site line will be highly useful. In addition to general benefits of landing site lines like reduction in time, cost and experimental animals, the assembly of the *attB*-containing U6 promoter cassette is

significantly simplified compared to the assembly of the entire construct containing the generic portion as well as the gene-specific *U6* promoter cassettes. Moreover, the 3C landing site line would be compatible with other transgenic approaches for the expression of gRNAs. Recently, a tRNA-based multiplex gRNA expression system was shown to express up to ten different gRNAs from one scaffold (Shiraki and Kawakami, 2018). Finally, the 3C landing site line would serve as the best possible control to a 3C landing site gene inactivation line because both lines utilize the same transgene integration site.

Another highly efficient system, termed CRISPR-Switch, also allows Cre-controlled CRISPR/Cas9 mutagenesis (Chylinski et al., 2019). However, in contrast to 3C mutagenesis, which enables the expression of Cas9 following a Cre recombination event, CRISPR-Switch controls the production of the gRNA in a Cre-dependent manner. In doing so, CRISPR-Switch allows even sequential gene editing of two loci in a temporal order, which is currently not possible with 3C mutagenesis. Despite this limitation, 3C mutagenesis has the potential for applications in other model organisms. In this context, we noted in the course of our studies that a similar system to 3C mutagenesis has been applied in mouse resulting in conditional gene inactivation (Chen et al., 2017). However, only low Cas9 expression was reported and moreover, although an in frame fusion with a FLAG tag allows subsequent identification of putative mutant cells via immunohistochemistry in fixed tissues, additional options like live imaging and FACS are not possible with the published design. We foresee that our 3C mutagenesis strategy will enable a variety of possible applications for conditional gene inactivation studies when used in combination with the appropriate Cre driver lines. In this context, recent efforts to increase the number of available Cre driver lines are now reinforced by new genome-editing approaches allowing the targeted knock-in of Cre or $CreER^{T2}$ at endogenous loci in the zebrafish genome providing novel Cre driver lines (Jungke et al., 2015; Kesavan et al., 2018). These novel lines, which reliably recapitulate endogenous gene expression patterns, will help to exploit the full potential of 3C mutagenesis.

Acknowledgments

We thank Drs. W.B. Chen and L. Zon for sharing reagents, M. Fischer, J. Michling and D. Mögel for excellent zebrafish care and Drs. R. Behrendt, S. Schulte-Merker and R. Kelsh for critically reading the manuscript. In addition, we thank the members of the Brand laboratory for continued support and discussions as well as helpful comments on the manuscript. This work was supported by the Light Microscopy Facility and Flow Cytometry Facility, core facilities of the CMCB at the Technische Universität Dresden. Funding was provided by the Technische Universität Dresden, the Deutsche Forschungsgemeinschaft to S.H. (HA 6362/2) and M.B. (BR 1746/3) and the European Union (European Research Council AdG Zf-BrainReg) to M.B. The funders had no role in study design, data collection and analysis, decision to publish, or preparation of the manuscript.

Materials and Methods

Ethical statement

Fish were kept according to FELASA guidelines (Aleström et al., 2020). All animal experiments were conducted according to the guidelines and under supervision of the Regierungspräsidium Dresden (permit: TVV 21/2018). All efforts were made to minimize animal suffering and the number of animals used.

Zebrafish husbandry and lines

Zebrafish were kept and bred according to standard procedures (Brand, 2002; Westerfield, 2000). Our experiments were carried out using zebrafish from wild-type stocks with the AB genetic background and the transgenic lines *Tg(otx2b:CreER^{T2})tud44*, abbreviated *otx2b*:CreER^{T2} (Kesavan et al., 2018) and *Tg(-4.7sox10:Cre)ba73* abbreviated *sox10*:Cre (Rodrigues et al., 2012). Combinations of the Cre driver lines with 3C *tyr* was conducted at least eight times with at least 20 double transgenic animals analyzed. All animals showing GFP expression also displayed pigmentation defects if the heat treatment was applied prior to onset of *tyr* expression.

Plasmid construction and germ line transformation

To create the pTol hsp70l:loxP-DsRed-loxP-Cas9-GFP; U6a:tyr plasmid, several intermediate steps were taken. Initially, the coding sequence of GFP was PCR amplified from pTol hsp70l:loxP-DsRed-GFP (Kroehne et al., 2011) with primers GFP-for (5′-TATAACCGGTGAGATCTCCTAAGAAGAAGAGAAAGGTGGTGAGCAAGGGCGAGGAGC-3′) and GFP-rev (5′-TATATCTAGACTCGAGGATCCGCTAGCGATACATTGATGAGTTT-3′) flanked by the unique restriction sites AgeI and XbaI, respectively. After digestion, the PCR product was cloned into the vector pT3TS nCas9n (addgene #46757) (Jao et al., 2013) replacing a 256 base pairs AgeI/XbaI fragment from the vector and giving rise to pT3TS nCas9n-GFP. Subsequently, Cas9-GFP was digested using NcoI following blunt-ending with Klenow and a second digest with NheI. The fragment was subsequently ligated into pTol hsp70l:loxP-DsRed-GFP digested with SmaI and NheI replacing GFP and giving rise to pTol hsp70l:loxP-DsRed-loxP-Cas9-GFP (addgene #158962). To generate the U6a gRNA expression cassette, the *U6a* promotor including a gRNA backbone was PCR amplified from pDestTol2CG2-U6:gRNA (addgene #63156) (Ablain et al., 2015) with primers U6a-for (5′-ATATGGTACCGGCGCGCCATATATCCCGGGGCGTCTTTTGTTCTGGTCATC-3′) and U6a-rev (5′-ATATGAGCTCATGCTAGCAAAAAAGCACCGACTCGGTGCC-3′) flanked by the unique restriction sites Acc65I and SacI, respectively. After digestion, the PCR product was cloned into the pBluescript giving rise to pBS U6a gRNA (addgene #158961). For the generation of pBS U6a tyr the two BseRI enzyme sites at the 5’ end of the gRNA scaffold and the annealed oligos (tyr-for 5’-GGACTGGAGGACTTCTGGGGGT-3’; tyr-rev 5’-CCCCAGAAGTCCTCCAGTCCGA-3’) covering the *tyrosinase* target site 5’-

GGACTGGAGGACTTCTGGGGAGG-3' (Jao et al., 2013) were used according to established protocols (Ablain et al., 2015). Finally, pBS U6a tyr was digested using AscI and NheI and ligated into pTol hsp70l:loxP-DsRed-loxP-Cas9-GFP giving rise to final pTol hsp70l:loxP-DsRed-loxP-Cas9-GFP; U6a:tyr plasmid which was subsequently used for germ line transformation. To this aim, plasmid DNA and transposase mRNA were injected into fertilized eggs (F0), raised to adulthood and crossed to AB wild-type fish as previously described (Kawakami, 2004). To identify transgenic carriers, undechorionated F1 embryos were heat shocked at 24 hpf and examined under a fluorescent microscope at 50 hpf. This way, eleven out twenty-one independent founders were identified and four founders were chosen to establish independent lines (referred as 3C *tyr*). For detection of the recombined and non-recombined 3C construct the forward primer hsp70l-for 5'-CCGCAGAGAAACTCAACCGAAGAGAAGC-3' and the reverse primer Cas9-rev 5'-GTTTCCAAAGATAGGATGGCGCTCG-3' were used in a standard PCR on genomic DNA (PCR parameters: 2 min at 95°C followed by 35 cycles with 30 sec at 95°C, 30 sec at 59°C and 30 sec at 72°C followed by 7 min at 72°C).

4-Hydroxytamoxifen, Cre mRNA and heat treatments

4-Hydroxytamoxifen (4OHT; Sigma, H7904) treatment was conducted as previously described (Hans et al., 2009). Briefly, embryos, still in their chorions, were transferred into petri dishes containing 4-OHT with a working concentration of 0.5µM at early gastrulation (shield or 6 hpf). For control treatments, sibling embryos were incubated in corresponding dilutions of ethanol. All incubations were conducted in the dark. Cre mRNA were conducted as previously described (Chekuru et al., 2017). Cre mRNA injections into 3C *tyr*-positive progeny at the 1-cell stage was conducted five times with at least 30 transgenic animals analyzed. All animals showing GFP expression also displayed pigmentation defects if the heat treatment was applied prior to onset of *tyr* expression. For heat treatments, embryos, still in their chorions, were transferred into fresh petri dishes. After removal of excess embryo medium, 42°C embryo medium was added and the petri dishes were kept for 30 minutes in a 37ºC incubator before they returned to a 28.5ºC incubator.

Imaging

Embryos and larvae were anesthetized with 0.01% MESAB (MS-222 or tricaine) in E3 medium and then mounted in 3% methylcellulose. Images were taken by a Olympus MVX microscope equipped with Olympus DP80 digital camera and the cellSens Dimension imaging software. Images were processed using Adobe Photoshop CC2015. Figures were assembled using Adobe Illustrator CC2015.

Tissue dissociation and fluorescence-activated cell sorting (FACS)

Tissue dissociation was conducted as described previously (Manoli and Driever, 2012). Briefly, embryos were removed from their chorions by pronase treatment (Westerfield, 2000),

followed by deyolking at 4°C in 0.5% Ginzburg-Ringer without $CaCl_2$. Dissociation was conducted in trypsin-EDTA on ice. When embryos were completely dissociated, the reaction was stopped by adding Hi-FBS. The cells were pelleted, washed with PBS, resuspended in PBS and passed through a 40 µM mesh filter prior to cell sorting. FACS was performed using an Aria II cell sorter (BD Biosciences). Forward and side scatter were used to gate for live, single cells, out of which GFP-positive cells were sorted and collected. For control cells from GFP-negative embryos the same gating strategy was employed. Flow cytometry data were analyzed using BD FACSDiva software. DNA was extracted from sorted cells using Quick-gDNA Miniprep Kit (Zymo Research, Cat. No.: D3025) following manufacturer's instructions for cell suspensions.

High-throughput single-end sequencing and CRISPR/Cas9 genotyping

Genomic DNA from individual embryos/larvae was extracted according to the “still quick, less dirty” protocol (Westerfield, 2000). The regions containing the *tyr* target or *tyr* off-target were amplified in a standard PCR (PCR parameters: 2 min at 95°C followed by 25 cycles with 30 sec at 95°C, 30 sec at 59°C and 30 sec at 72°C followed by 7 min at 72°C) using tyr-P5-tail 5’-CACTCTTTCCCTACACGACGCTCTTCCGATCTGCCGGGCCAGACTGGACAGC-3’ and tyr-P7-tail 5’-GTGACTGGAGTTCAGACGTGTGCTCTTCCGATCTGCCTCTCACTCTCCTCGACTCTTC-3’ or tyr-off-P5-tail 5’-ACACTCTTTCCCTACACGACGCTCTTCCGATCTGGCAGACGGGTGAATTAGTGATGC-3’ and tyr-off-P7-tail 5’-GTGACTGGAGTTCAGACGTGTGCTCTTCCGATCTAGCCAAGACTTGAACCAGCGAGC-3’, respectively. After amplification, PCR products were purified using NuceloSpin Gel and PCR Clean-up (Macherey Nagel, 740609.250) following the manufacturer's instructions. In order to sequence the CRISPR PCR products, an 8-cycle index PCR with Illumina TruSeq-primer was run with 2 ng starting material. Libraries were quantified, and 75 bp single-end reads were sequenced on the Illumina NextSeq 500 platform to a minimum depth of 4 million reads. We used the tool CRISPResso2 (Clement et al., 2019) to trim sequencing adapters, align sequencing reads to the amplified PCR sequence, quantify the number of insertions, substitutions and deletions in the reads, and finally visualize the results. Default parameters were applied with the exception of *--trim_sequences* and *--trimmomatic_options_string* to trim sequencing adapters, *--quantification_window_size 10*, and *--exclude_bp_from_left 0 --exclude_bp_from_right 0*.

References

Ablain, J., Durand, Ellen M., Yang, S., Zhou, Y., Zon, Leonard I., 2015. A CRISPR/Cas9 Vector System for Tissue-Specific Gene Disruption in Zebrafish. Developmental Cell 32, 756-764.

Aleström, P., D'Angelo, L., Midtlyng, P.J., Schorderet, D.F., Schulte-Merker, S., Sohm, F., Warner, S., 2020. Zebrafish: Housing and husbandry recommendations. Lab Anim 54, 213-224.

Auer, T.O., Duroure, K., De Cian, A., Concordet, J.-P., Del Bene, F., 2013. Highly efficient CRISPR/Cas9-mediated knock-in in zebrafish by homology-independent DNA repair. Genome Research.

Becher, B., Waisman, A., Lu, L.-F., 2018. Conditional Gene-Targeting in Mice: Problems and Solutions. Immunity 48, 835-836.

Bedell, V.M., Wang, Y., Campbell, J.M., Poshusta, T.L., Starker, C.G., Krug Ii, R.G., Tan, W., Penheiter, S.G., Ma, A.C., Leung, A.Y.H., Fahrenkrug, S.C., Carlson, D.F., Voytas, D.F., Clark, K.J., Essner, J.J., Ekker, S.C., 2012. In vivo genome editing using a high-efficiency TALEN system. Nature 491, 114-118.

Botstein, D., Fink, G., 1988. Yeast: an experimental organism for modern biology. 240, 1439-1443.

Brand, M., Granato, M., and Nüsslein-Volhard, C. , 2002. Keeping and raising zebrafish. In Zebrafish, A Practical Approach. Oxford , Oxford University Press;, 7-37.

Brenner, S., 1974. THE GENETICS OF CAENORHABDITIS ELEGANS. 77, 71-94.

Burg, L., Palmer, N., Kikhi, K., Miroshnik, E.S., Rueckert, H., Gaddy, E., MacPherson Cunningham, C., Mattonet, K., Lai, S.-L., Marín-Juez, R., Waring, R.B., Stainier, D.Y.R., Balciunas, D., 2018. Conditional mutagenesis by oligonucleotide-mediated integration of loxP sites in zebrafish. PLOS Genetics 14, e1007754.

Camp, E., Lardelli, M., 2001. Tyrosinase gene expression in zebrafish embryos. Development genes and evolution 211, 150-153.

Capecchi, M.R., 2005. Gene targeting in mice: functional analysis of the mammalian genome for the twenty-first century. Nature Reviews Genetics 6, 507-512.

Cerda, G.A., Thomas, J.E., Allende, M.L., Karlstrom, R.O., Palma, V., 2006. Electroporation of DNA, RNA, and morpholinos into zebrafish embryos. Methods (San Diego, Calif 39, 207-211.

Chekuru, A., Kuscha, V., Hans, S., Brand, M., 2017. Ligand-Controlled Site-Specific Recombination in Zebrafish, in: Eroshenko, N. (Ed.), Site-Specific Recombinases: Methods and Protocols. Springer New York, New York, NY, pp. 87-97.

Chen, J., Du, Y., He, X., Huang, X., Shi, Y.S., 2017. A Convenient Cas9-based Conditional Knockout Strategy for Simultaneously Targeting Multiple Genes in Mouse. Scientific Reports 7, 517.

Chylinski, K., Hubmann, M., Hanna, R.E., Yanchus, C., Michlits, G., Uijttewaal, E.C.H., Doench, J., Schramek, D., Elling, U., 2019. CRISPR-Switch regulates sgRNA activity by Cre recombination for sequential editing of two loci. Nature Communications 10, 5454.

Clement, K., Rees, H., Canver, M.C., Gehrke, J.M., Farouni, R., Hsu, J.Y., Cole, M.A., Liu, D.R., Joung, J.K., Bauer, D.E., Pinello, L., 2019. CRISPResso2 provides accurate and rapid genome editing sequence analysis. Nature biotechnology 37, 224-226.

Cubbon, A., Ivancic-Bace, I., Bolt, E.L., 2018. CRISPR-Cas immunity, DNA repair and genome stability. Biosci Rep 38, BSR20180457.

Feil, R., 2007. Conditional somatic mutagenesis in the mouse using site-specific recombinases. Handbook of experimental pharmacology, 3-28.

Gaj, T., Gersbach, C.A., Barbas, C.F., III, 2013. ZFN, TALEN, and CRISPR/Cas-based methods for genome engineering. Trends in Biotechnology 31, 397-405.

Halloran, M.C., Sato-Maeda, M., Warren, J.T., Su, F., Lele, Z., Krone, P.H., Kuwada, J.Y., Shoji, W., 2000. Laser-induced gene expression in specific cells of transgenic zebrafish. Development 127, 1953-1960.

Hans, S., Freudenreich, D., Geffarth, M., Kaslin, J., Machate, A., Brand, M., 2011. Generation of a non-leaky heat shock–inducible Cre line for conditional Cre/lox strategies in zebrafish. Developmental Dynamics 240, 108-115.

Hans, S., Kaslin, J., Freudenreich, D., Brand, M., 2009. Temporally-Controlled Site-Specific Recombination in Zebrafish. PLoS ONE 4, e4640.

Hirsh, D., Vanderslice, R., 1976. Temperature-sensitive developmental mutants of Caenorhabditis elegans. Developmental Biology 49, 220-235.

Hoshijima, K., Jurynec, M.J., Grunwald, D.J., 2016. Precise Editing of the Zebrafish Genome Made Simple and Efficient. Developmental cell 36, 654-667.

Jao, L.-E., Wente, S.R., Chen, W., 2013. Efficient multiplex biallelic zebrafish genome editing using a CRISPR nuclease system. Proceedings of the National Academy of Sciences 110, 13904-13909.

587 Jungke, P., Hammer, J., Hans, S., Brand, M., 2015. Isolation of Novel CreERT2-Driver Lines in
588 Zebrafish Using an Unbiased Gene Trap Approach. PloS one 10, e0129072-e0129072.
589 Kawakami, K., 2004. Transgenesis and gene trap methods in zebrafish by using the Tol2 transposable
590 element. Methods in cell biology 77, 201-222.
591 Kesavan, G., Hammer, J., Hans, S., Brand, M., 2018. Targeted knock-in of CreERT2in zebrafish using
592 CRISPR/Cas9. Cell and Tissue Research 372, 41-50.
593 Kesavan, G., Machate, A., Hans, S., Brand, M., 2020. Cell-fate plasticity, adhesion and cell sorting
594 complementarily establish a sharp midbrain-hindbrain boundary. 147, dev186882.
595 Kroehne, V., Freudenreich, D., Hans, S., Kaslin, J., Brand, M., 2011. Regeneration of the adult zebrafish
596 brain from neurogenic radial glia-type progenitors. Development 138, 4831-4841.
597 Labun, K., Montague, T.G., Krause, M., Torres Cleuren, Y.N., Tjeldnes, H., Valen, E., 2019.
598 CHOPCHOP v3: expanding the CRISPR web toolbox beyond genome editing. Nucleic Acids Research
599 47, W171-W174.
600 Li, W., Zhang, Y., Han, B., Li, L., Li, M., Lu, X., Chen, C., Lu, M., Zhang, Y., Jia, X., Zhu, Z., Tong, X.,
601 Zhang, B., 2019. One-step efficient generation of dual-function conditional knockout and geno-tagging
602 alleles in zebrafish. eLife 8, e48081.
603 Manoli, M., Driever, W., 2012. Fluorescence-activated cell sorting (FACS) of fluorescently tagged cells
604 from zebrafish larvae for RNA isolation. Cold Spring Harbor protocols 2012.
605 Mosimann, C., Puller, A.-C., Lawson, K.L., Tschopp, P., Amsterdam, A., Zon, L.I., 2013. Site-directed
606 zebrafish transgenesis into single landing sites with the phiC31 integrase system. Developmental
607 Dynamics 242, 949-963.
608 Nüsslein-Volhard, C., 2012. The zebrafish issue of Development. 139, 4099-4103.
609 Nüsslein-Volhard, C., Wieschaus, E., 1980. Mutations affecting segment number and polarity in
610 Drosophila. Nature 287, 795-801.
611 Rodrigues, F.S., Doughton, G., Yang, B., Kelsh, R.N., 2012. A novel transgenic line using the Cre-lox
612 system to allow permanent lineage-labeling of the zebrafish neural crest. Genesis 50, 750-757.
613 Shah, A.N., Davey, C.F., Whitebirch, A.C., Miller, A.C., Moens, C.B., 2015. Rapid reverse genetic
614 screening using CRISPR in zebrafish. Nature methods 12, 535-540.
615 Shin, J., Chen, J., Solnica-Krezel, L., 2014. Efficient homologous recombination-mediated genome
616 engineering in zebrafish using TALE nucleases. 141, 3807-3818.
617 Shiraki, T., Kawakami, K., 2018. A tRNA-based multiplex sgRNA expression system in zebrafish and
618 its application to generation of transgenic albino fish. Scientific Reports 8, 13366.
619 Suzuki, D.T., 1970. Temperature-Sensitive Mutations in Drosophila melanogaster. Science 170, 695-
620 706.
621 Westerfield, M., 2000. The zebrafish book. A guide for the laboratory use of zebrafish (Danio rerio). 4th
622 ed., Univ. of Oregon Press, Eugene.
623 Wu, R.S., Lam, I.I., Clay, H., Duong, D.N., Deo, R.C., Coughlin, S.R., 2018. A Rapid Method for Directed
624 Gene Knockout for Screening in G0 Zebrafish. Developmental Cell 46, 112-125.e114.
625 Yarmolinsky, M., Hoess, R., 2015. The Legacy of Nat Sternberg: The Genesis of Cre-lox Technology.
626 Annual review of virology 2, 25-40.
627 Yin, L., Maddison, L.A., Li, M., Kara, N., LaFave, M.C., Varshney, G.K., Burgess, S.M., Patton, J.G.,
628 Chen, W., 2015. Multiplex Conditional Mutagenesis Using Transgenic Expression of Cas9 and sgRNAs.
629 Genetics 200, 431-441.
630 Zou, M., De Koninck, P., Neve, R.L., Friedrich, R.W., 2014. Fast gene transfer into the adult zebrafish
631 brain by herpes simplex virus 1 (HSV-1) and electroporation: methods and optogenetic applications.
632 Frontiers in neural circuits 8, 41-41.
633

Figures

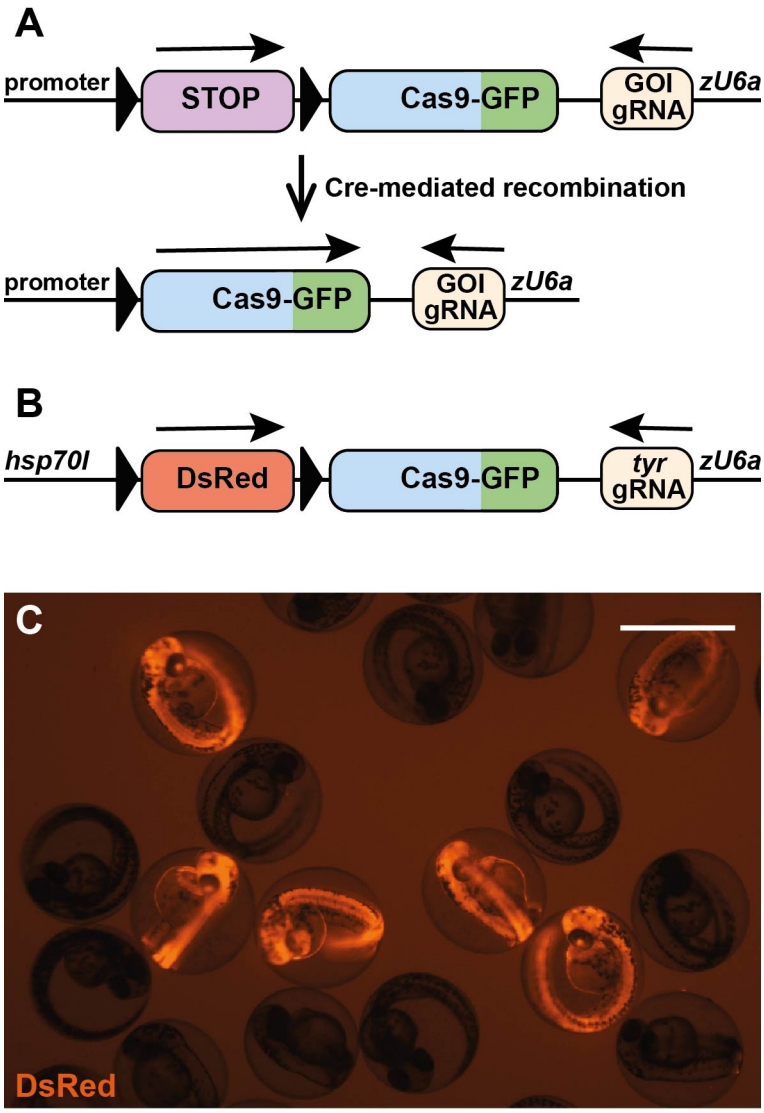

Figure 1: Cre-Controlled CRISPR (3C) mutagenesis allows gene inactivation in Cre-dependent manner. (A) Scheme of the rationale of 3C. A Cre effector construct controls the expression of a floxed Stop cassette upstream of the sequence encoding a fusion protein of Cas9 and GFP. In addition, a *U6a* promoter drives the constitutive expression of a gRNA targeting a gene of interest (GOI). In the absence of Cre, only the gRNA is present but no Cas9-GFP. Consequently, mutagenesis does not occur and the gene of interest remains intact. After Cre-mediated recombination, expression of Cas9-GFP and the gRNA allows the formation of a functional CRISPR complex and results in mutagenesis of the target site within the gene of interest. (B) Scheme of the 3C gene inactivation construct targeting *tyrosinase* (*tyr*). The temperature-inducible *hsp70l* promotor drives expression of a floxed DsRed cassette. (C) Identification of transgenic animals expressing DsRed at 50 hpf after a heat treatment at 24 hpf. Scale bar: 1000 µm.

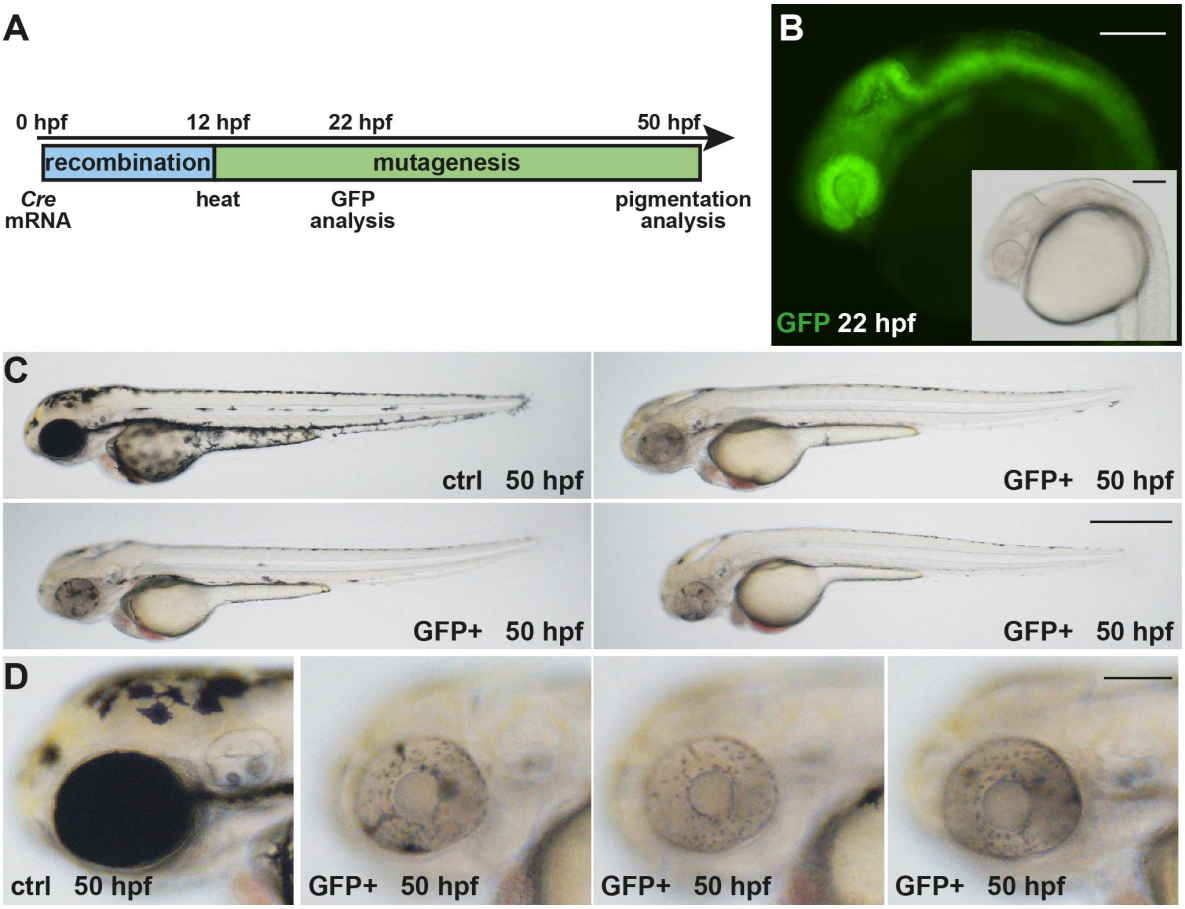

Figure 2: Cre mRNA injections into 3C *tyr* result in ubiquitous GFP expression and widespread pigmentation defects. (A) Timeline. Cre mRNA injections at the 1-cell stage elicit ubiquitous recombination (blue box). At 12 hpf, a heat treatment triggers transient Cas9-GFP expression causing the subsequent permanent mutagenesis of the *tyr* target site (green box). Analysis of GFP expression and pigmentation was conducted at 22 and 50 hpf, respectively. (B) Expression of GFP is detected in a ubiquitous fashion at 22 hpf. (C, D) In comparison to controls (ctrl), GFP-positive embryos (GFP+) display a significant loss of black pigment along the body (C) and in the developing eye (D). Scale bars: 150 µm in B and D; 500 µm in C.

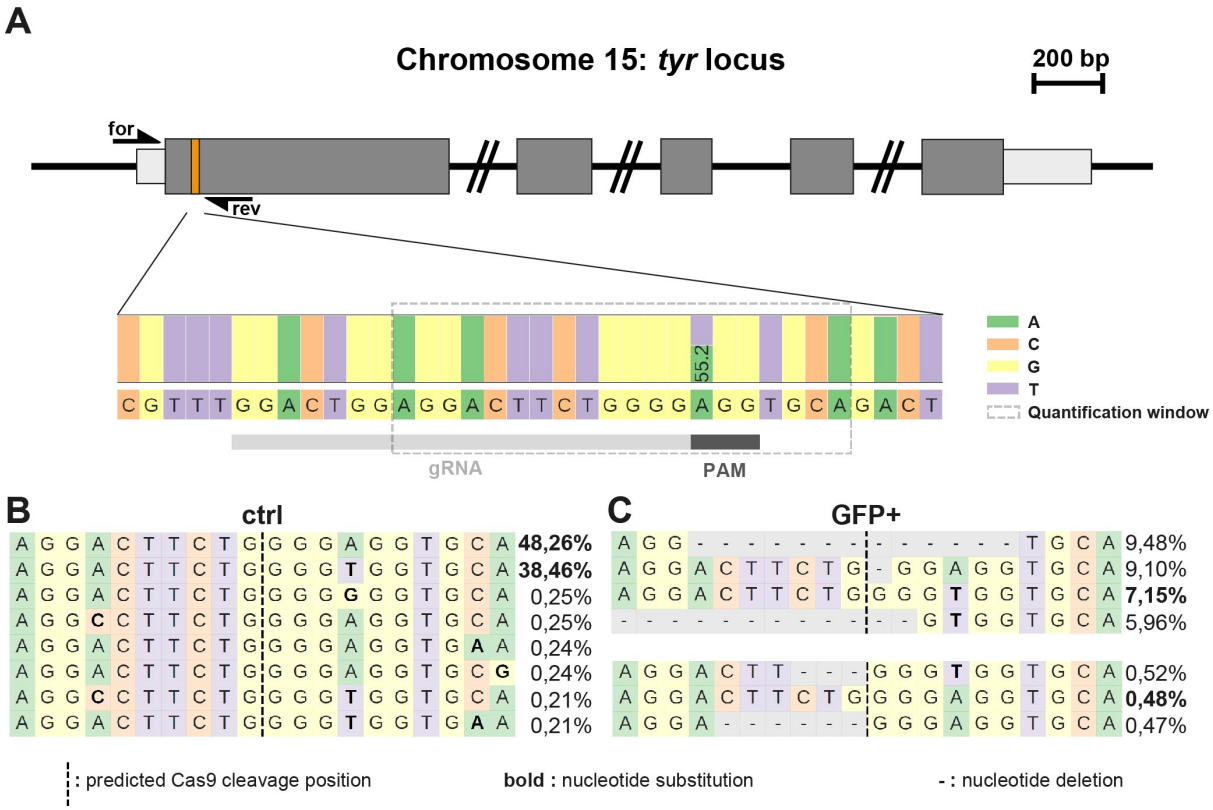

Figure 3: Sequencing confirms high mutagenesis rates following Cas9-GFP expression. (A) Scheme of the *tyr* locus at chromosome 15. Exon sequences with translated and untranslated regions are represented in dark and light grey, respectively. Position of the CRISPR/Cas9 target in the first exon is indicated with an orange box. Forward and reverse primers used for amplification of the target site (for and rev) are shown as half arrows. Scale bar: 200 base pairs (bp). Next generation sequencing of FAC-sorted cells from pooled embryos (see Suppl. Fig. 1A) revealed a single nucleotide polymorphism at the first position of the protospacer adjacent motif (PAM) indicated with a dark grey box downstream to the target site (gRNA) indicated by a light grey box. (B, C) Distribution of identified alleles around the cleavage site for the guide GGACTGGAGGACTTCTGGGG in control (ctrl) and GFP-positive cells (GFP+). Nucleotides are indicated by unique colors (A = green; C = red; G = yellow; T = purple). Substitutions are shown in bold font. Horizontal dashed lines indicate deleted sequences. The vertical dashed line indicates the predicted cleavage site. Sequencing of controls (B) shows presence of the parental strands with a frequency of 48.26% and 38.46% which drops to 7.15% and 0.48% in GFP-positive cells (C).

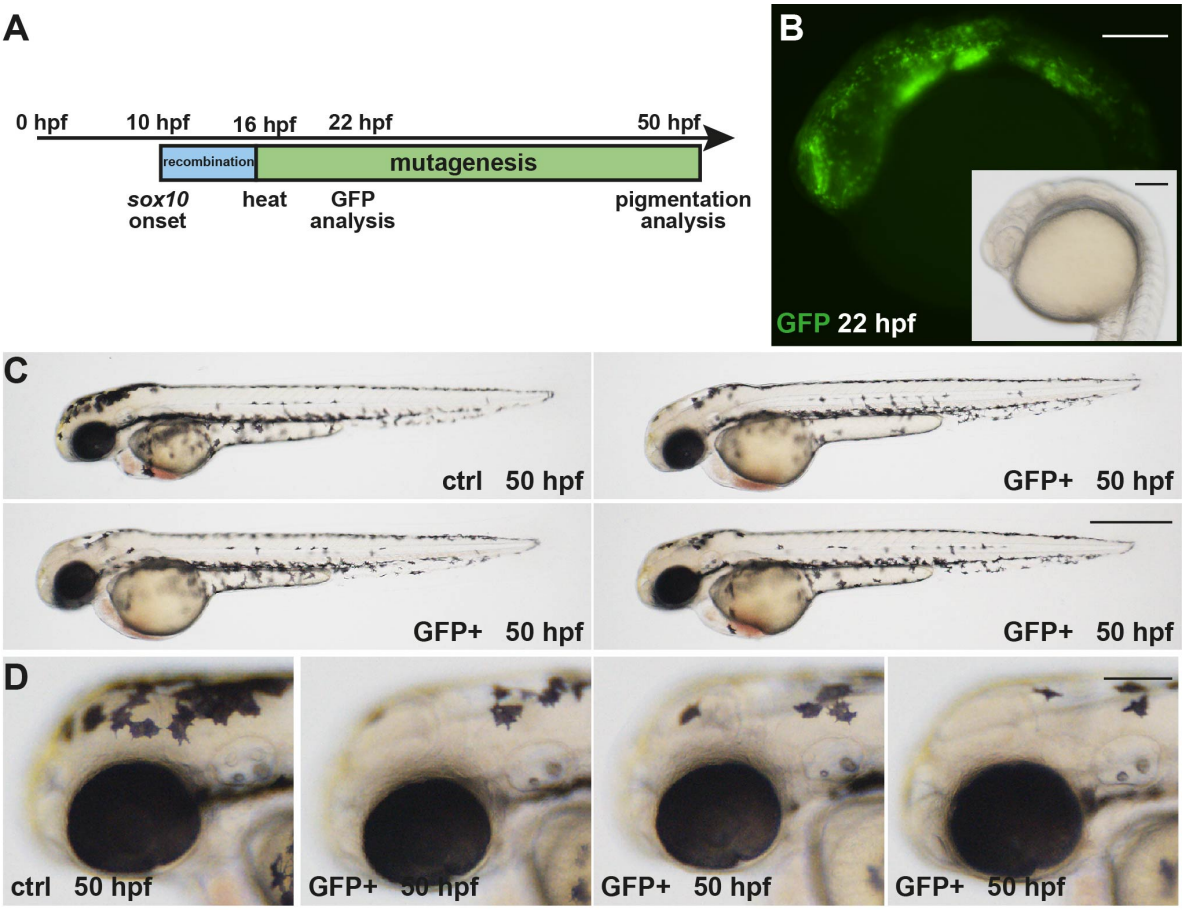

676

677 **Figure 4: *sox10*-specific Cre activity results in spatiotemporally-controlled GFP**
678 **expression and pigmentation defects along the body.** (A) Timeline. Cre activity in
679 *sox10*:Cre-positive animals at 10 hpf elicits recombination (blue box) in developing neural
680 crest cells. At 16 hpf, a heat treatment triggers expression of Cas9-GFP and the subsequent
681 permanent mutagenesis of the *tyr* target site (green box). Analysis of GFP expression and
682 pigmentation was conducted at 22 and 50 hpf, respectively. (B) Expression of GFP is detected
683 in neural crest cells at 22 hpf. (C, D) In comparison to controls (ctrl), GFP-positive embryos
684 (GFP+) display a loss of pigmentation in the anterior head region. Scale bars: 150 µm in B
685 and D; 500 µm in C.

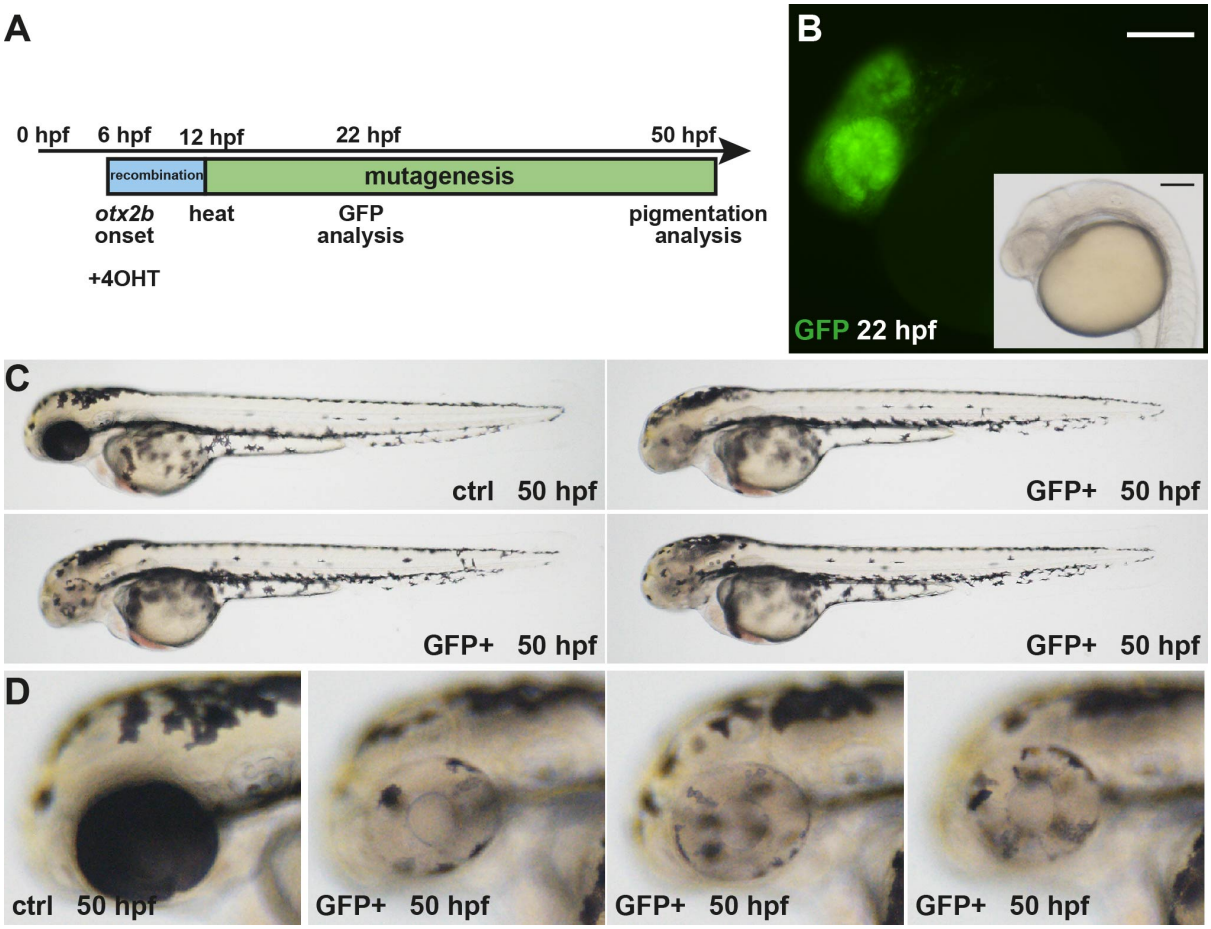

Figure 5: *otx2b*-specific Cre activity results in spatiotemporally-controlled GFP expression and pigmentation defects in the developing eyes.

(A) Timeline. Application of 4-Hydroxytamoxifen (4OHT) induces Cre activity in *otx2b*:CreER^{T2}-positive animals at 6 hpf eliciting recombination (blue box) in cells of the developing anterior neural plate. At 12 hpf, a heat treatment triggers expression of Cas9-GFP and the subsequent mutagenesis of the *tyr* target site (green box). Analysis of GFP expression and pigmentation was conducted at 22 and 50 hpf, respectively. (B) Expression of GFP is detected in cells of the developing fore-, midbrain and eyes at 22 hpf. (C, D) In comparison to controls (ctrl), GFP-positive embryos (GFP+) display no pigmentation loss in cells along the body, but significant pigmentation defects in the developing eyes. Scale bars: 150 µm in B and D; 500 µm in C.

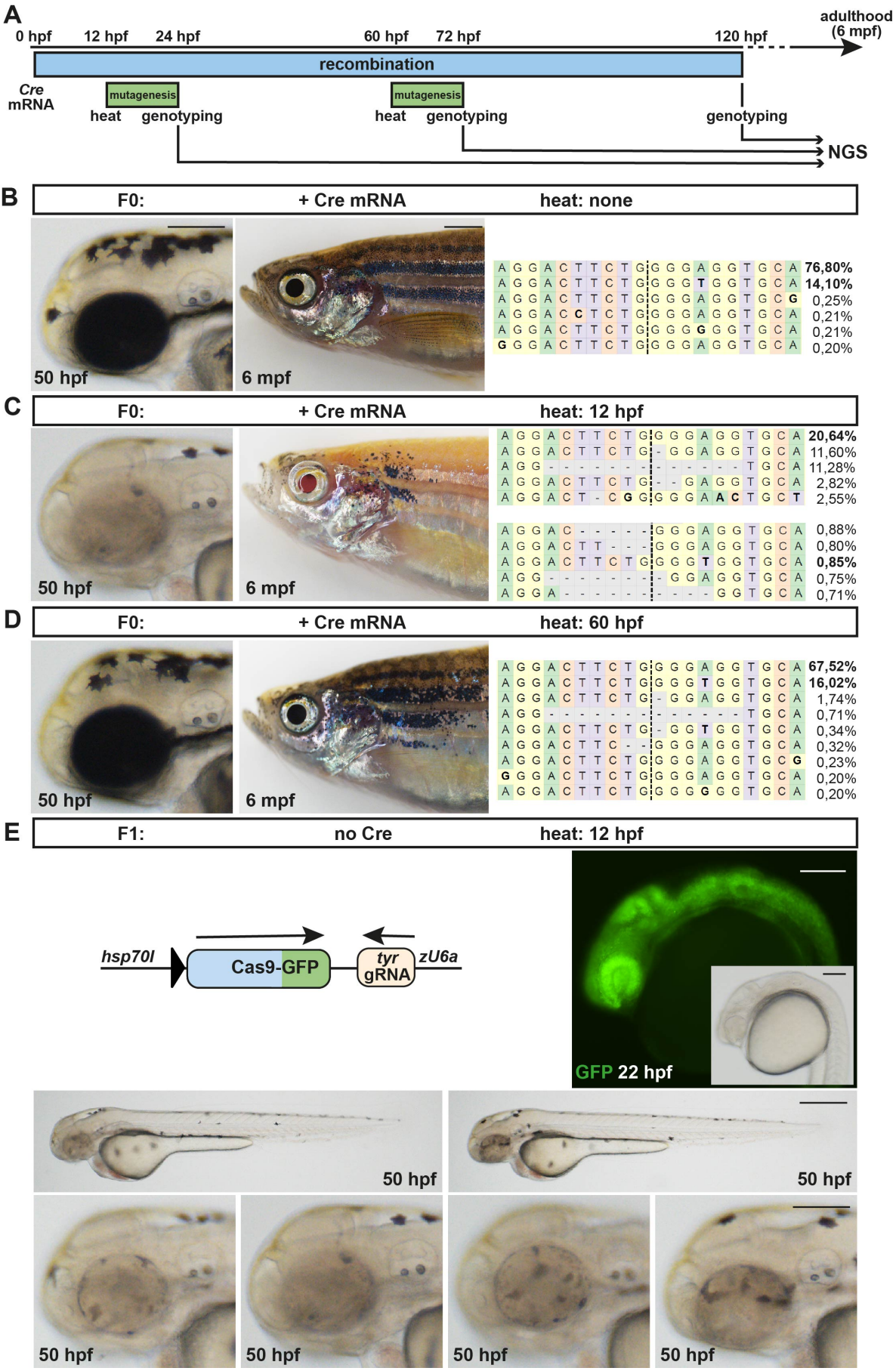
A
0 hpf
12 hpf
24 hpf
60 hpf
72 hpf
120 hpf
adulthood
(6 mpf)
recombination
Cre
mRNA
mutagenesis
heat
genotyping
mutagenesis
heat
genotyping
genotyping
NGS
B
F0:
+ Cre mRNA
heat: none
50 hpf
6 mpf
76,80%
14,10%
0,25%
0,21%
0,21%
0,20%
C
F0:
+ Cre mRNA
heat: 12 hpf
50 hpf
6 mpf
20,64%
11,60%
11,28%
2,82%
2,55%
0,88%
0,80%
0,85%
0,75%
0,71%
D
F0:
+ Cre mRNA
heat: 60 hpf
50 hpf
6 mpf
67,52%
16,02%
1,74%
0,71%
0,34%
0,32%
0,23%
0,20%
0,20%
E
F1:
no Cre
heat: 12 hpf
hsp70l
Cas9-GFP
tyr
gRNA
zU6a
GFP 22 hpf
50 hpf
50 hpf
50 hpf
50 hpf
50 hpf
50 hpf

699

Figure 6: Temporally-controlled gene inactivation. (A) Timeline. Cre mRNA injections into progeny of 3C *tyr* animals at the 1-cell stage elicit ubiquitous recombination (blue box). A subset of injected embryos was heat treated at 12 or 60 hpf to trigger Cas9-GFP expression and mutagenesis of the *tyr* target site (green box). In addition, Cre mRNA injected animals were collected at 120 hpf without a prior heat treatment. Single embryo genotyping was applied to all specimen and ten embryos of each time point (heat: none; heat: 12 hpf; heat 60 hpf) were combined and analyzed using next generation sequencing (NGS). In addition, siblings of all three time points were raised to adulthood (6 months post fertilization (mpf)). (B) Animals subjected to Cre mRNA injection but no heat treatment show neither a pigmentation phenotype at embryonic or adult stages nor any signs of mutagenesis. (C) A strong pigmentation phenotype is observed at embryonic (50 hpf) and adult stages (6 mpf) in animals heat treated at 12 hpf. (Note almost complete absence of pigmentation in the RPE at 6 mpf making the eye appear red.) NGS confirms high level indel production. (D) Pigmentation defects are observed at adult but not at embryonic stages in animals heat treated at 60 hpf. Sequencing corroborates mutagenesis of the *tyr* target site. (E) The recombined 3C *tyr* allele is transmitted in the germline of F0 animals subjected to Cre mRNA injection only. Heat treatment in the F1 generation results in GFP expression and pigmentation defects after activation at 12 hpf. Scale bars: 500 µm for 50 hpf and 2 mm for 6 mpf in B-D; 150 µm in E, except for lower row with 500 µm.

Figures

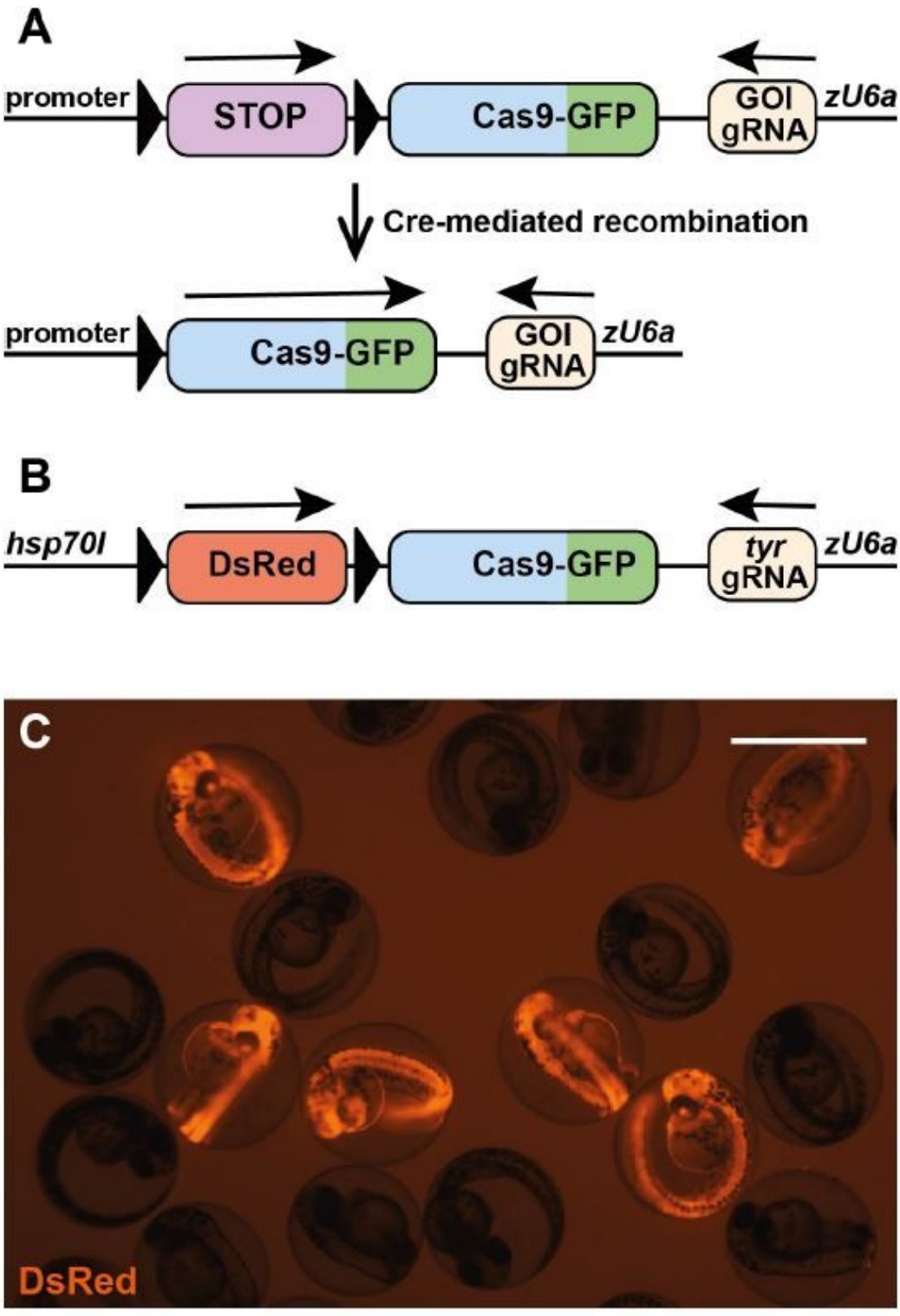

Figure 1

Cre-Controlled CRISPR (3C) mutagenesis allows gene inactivation in Cre-dependent manner. (A) Scheme of the rationale of 3C. A Cre effector construct controls the expression of a floxed Stop cassette upstream of the sequence encoding a fusion protein of Cas9 and GFP. In addition, a U6a promoter drives the

constitutive expression of a gRNA targeting a gene of interest (GOI). In the absence of Cre, only the gRNA is present but no Cas9-GFP. Consequently, mutagenesis does not occur and the gene of interest remains intact. After Cre-mediated recombination, expression of Cas9-GFP and the gRNA allows the formation of a functional CRISPR complex and results in mutagenesis of the target site within the gene of interest. (B) Scheme of the 3C gene inactivation construct targeting tyrosinase (tyr). The temperature-inducible hsp70l promotor drives expression of a floxed DsRed cassette. (C) Identification of transgenic animals expressing DsRed at 50 hpf after a heat treatment at 24 hpf. Scale bar: 1000 µm.

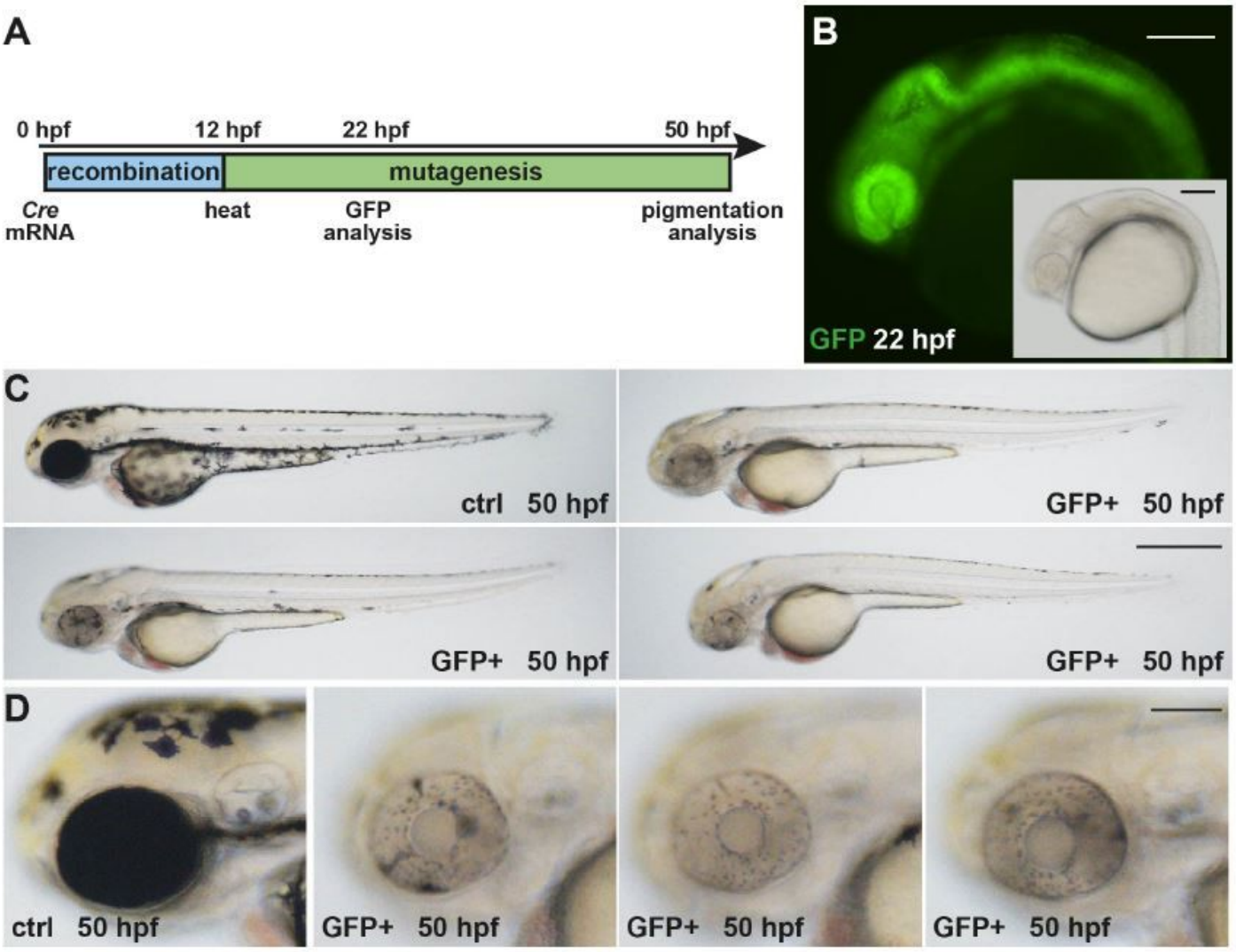

Figure 2

Cre mRNA injections into 3C tyr result in ubiquitous GFP expression and widespread pigmentation defects. (A) Timeline. Cre mRNA injections at the 1-cell stage elicit ubiquitous recombination (blue box). At 12 hpf, a heat treatment triggers transient Cas9-GFP expression causing the subsequent permanent mutagenesis of the tyr target site (green box). Analysis of GFP expression and pigmentation was conducted at 22 and 50 hpf, respectively. (B) Expression of GFP is detected in a ubiquitous fashion at 22 hpf. (C, D) In comparison to controls (ctrl), GFP-positive embryos (GFP+) display a significant loss of

black pigment along the body (C) and in the developing eye (D). Scale bars: 150 µm in B and D; 500 µm in C.

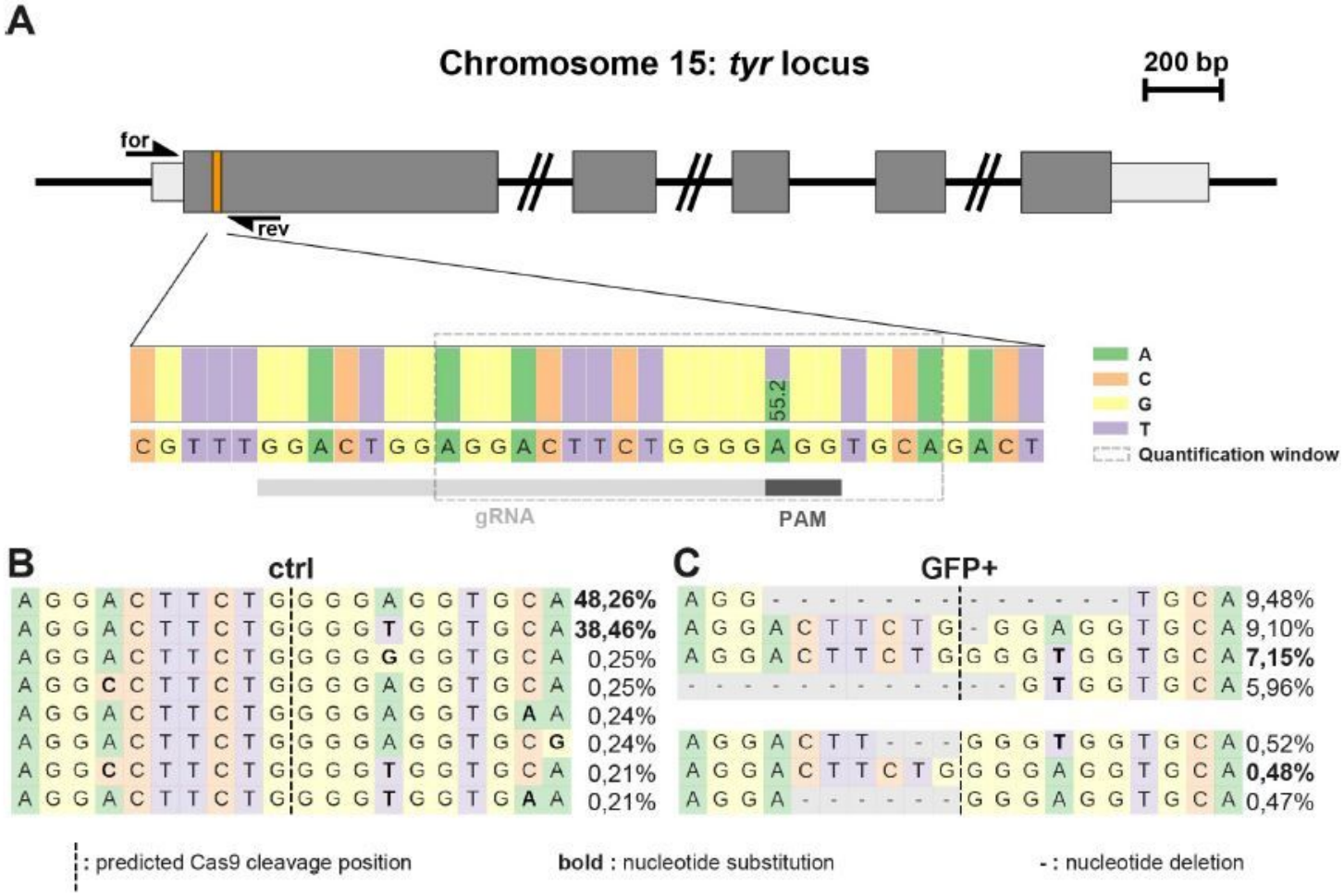

Figure 3

Sequencing confirms high mutagenesis rates following Cas9-GFP expression. (A) Scheme of the tyr locus at chromosome 15. Exon sequences with translated and untranslated regions are represented in dark and light grey, respectively. Position of the CRISPR/Cas9 target in the first exon is indicated with an orange box. Forward and reverse primers used for amplification of the target site (for and rev) are shown as half arrows. Scale bar: 200 base pairs (bp). Next generation sequencing of FAC-sorted cells from pooled embryos (see Suppl. Fig. 1A) revealed a single nucleotide polymorphism at the first position of the protospacer adjacent motif (PAM) indicated with a dark grey box downstream to the target site (gRNA) indicated by a light grey box. (B, C) Distribution of identified alleles around the cleavage site for the guide GGACTGGAGGACTTCTGGGG in control (ctrl) and GFP-positive cells (GFP+). Nucleotides are indicated by unique colors (A = green; C = red; G = yellow; T = purple). Substitutions are shown in bold font. Horizontal dashed lines indicate deleted sequences. The vertical dashed line indicates the predicted cleavage site. Sequencing of controls (B) shows presence of the parental strands with a frequency of 48.26% and 38.46% which drops to 7.15% and 0.48% in GFP-positive cells (C).

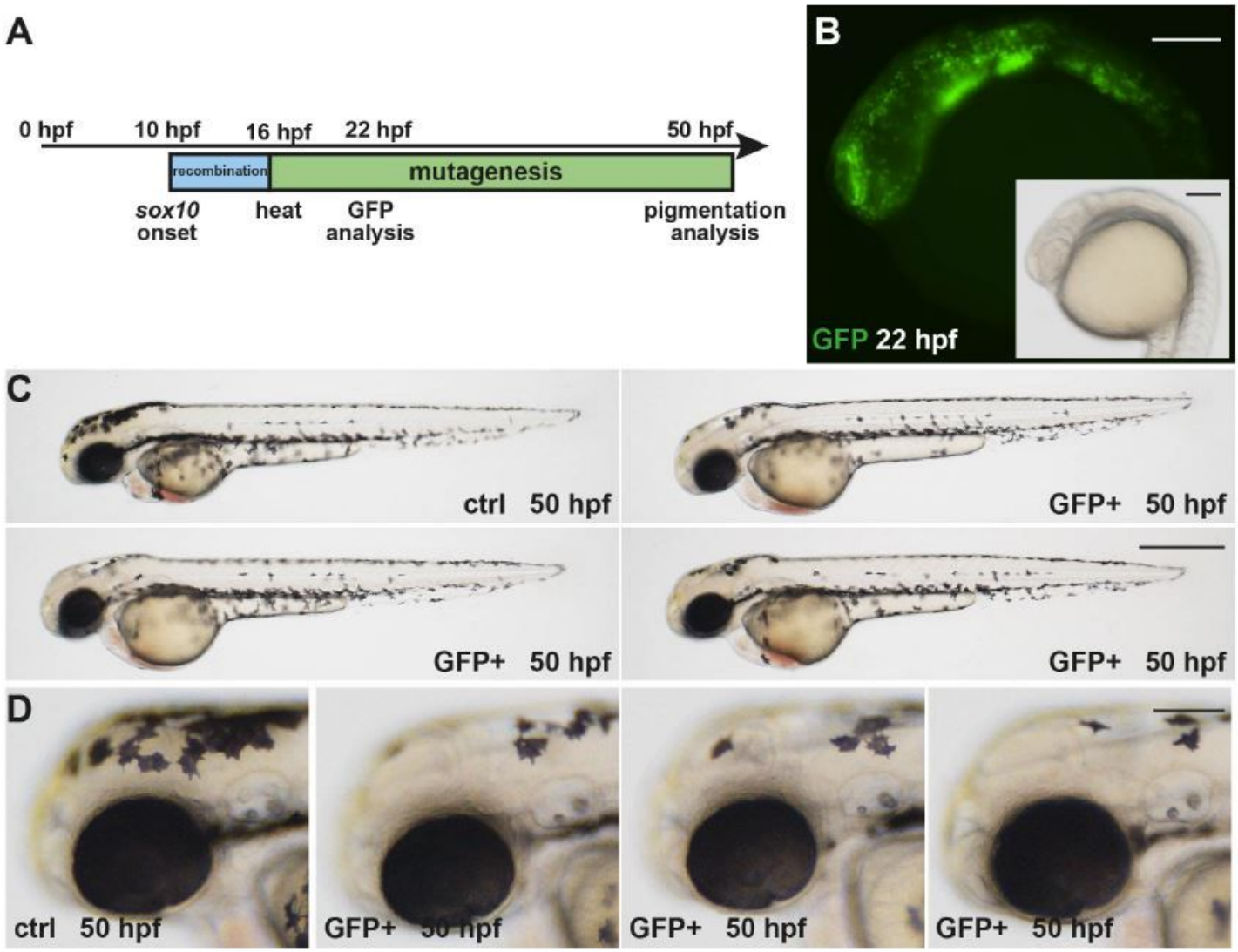

Figure 4

sox10-specific Cre activity results in spatiotemporally-controlled GFP expression and pigmentation defects along the body. (A) Timeline. Cre activity in sox10:Cre-positive animals at 10 hpf elicits recombination (blue box) in developing neural crest cells. At 16 hpf, a heat treatment triggers expression of Cas9-GFP and the subsequent permanent mutagenesis of the tyr target site (green box). Analysis of GFP expression and pigmentation was conducted at 22 and 50 hpf, respectively. (B) Expression of GFP is detected in neural crest cells at 22 hpf. (C, D) In comparison to controls (ctrl), GFP-positive embryos (GFP+) display a loss of pigmentation in the anterior head region. Scale bars: 150 µm in B and D; 500 µm in C.

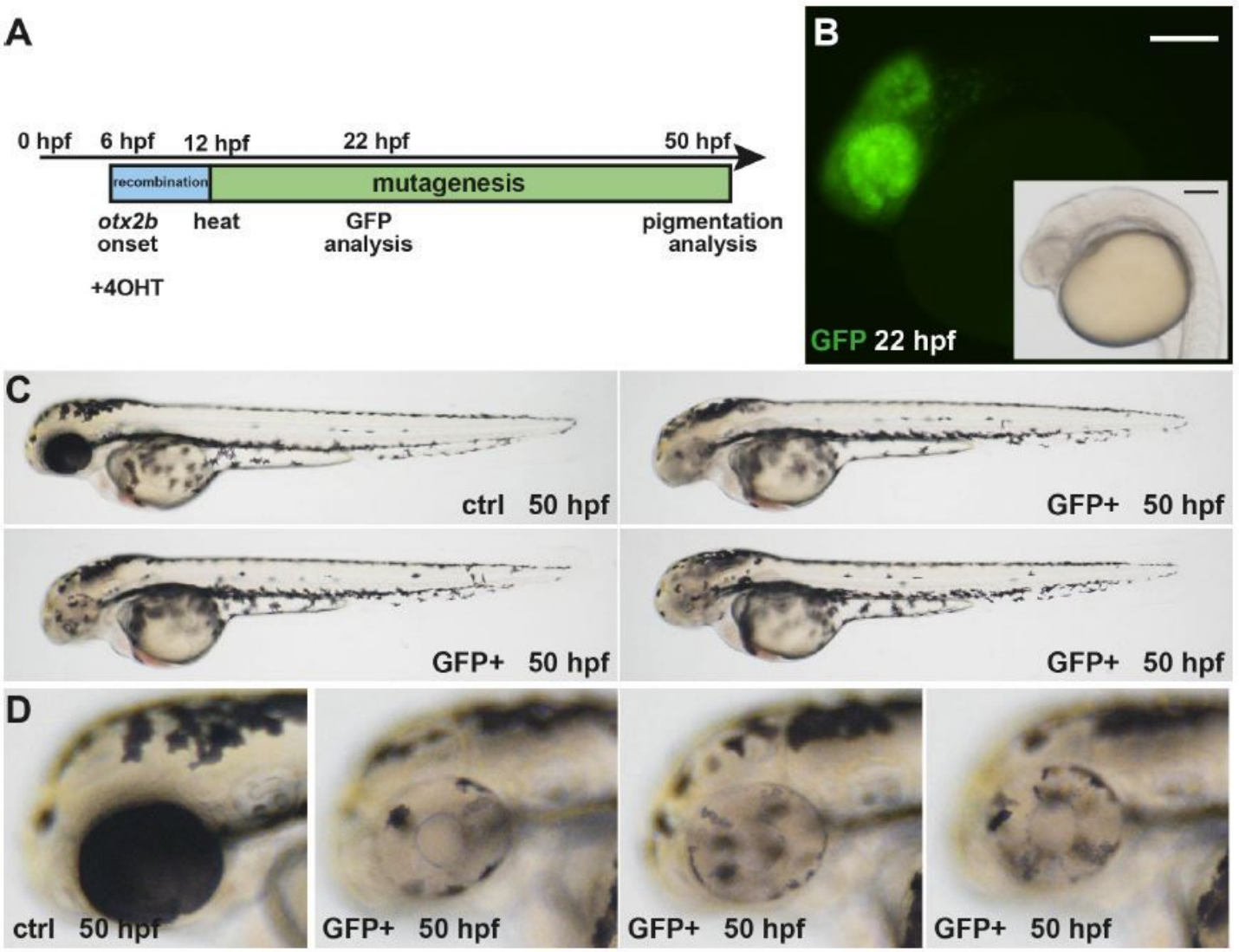

Figure 5

otx2b-specific Cre activity results in spatiotemporally-controlled GFP expression and pigmentation defects in the developing eyes. (A) Timeline. Application of 4-Hydroxytamoxifen (4OHT) induces Cre activity in otx2b:CreERT2-positive animals at 6 hpf eliciting recombination (blue box) in cells of the developing anterior neural plate. At 12 hpf, a heat treatment triggers expression of Cas9-GFP and the subsequent mutagenesis of the tyr target site (green box). Analysis of GFP expression and pigmentation was conducted at 22 and 50 hpf, respectively. (B) Expression of GFP is detected in cells of the developing fore-, midbrain and eyes at 22 hpf. (C, D) In comparison to controls (ctrl), GFP-positive embryos (GFP+) display no pigmentation loss in cells along the body, but significant pigmentation defects in the developing eyes. Scale bars: 150 µm in B and D; 500 µm in C.

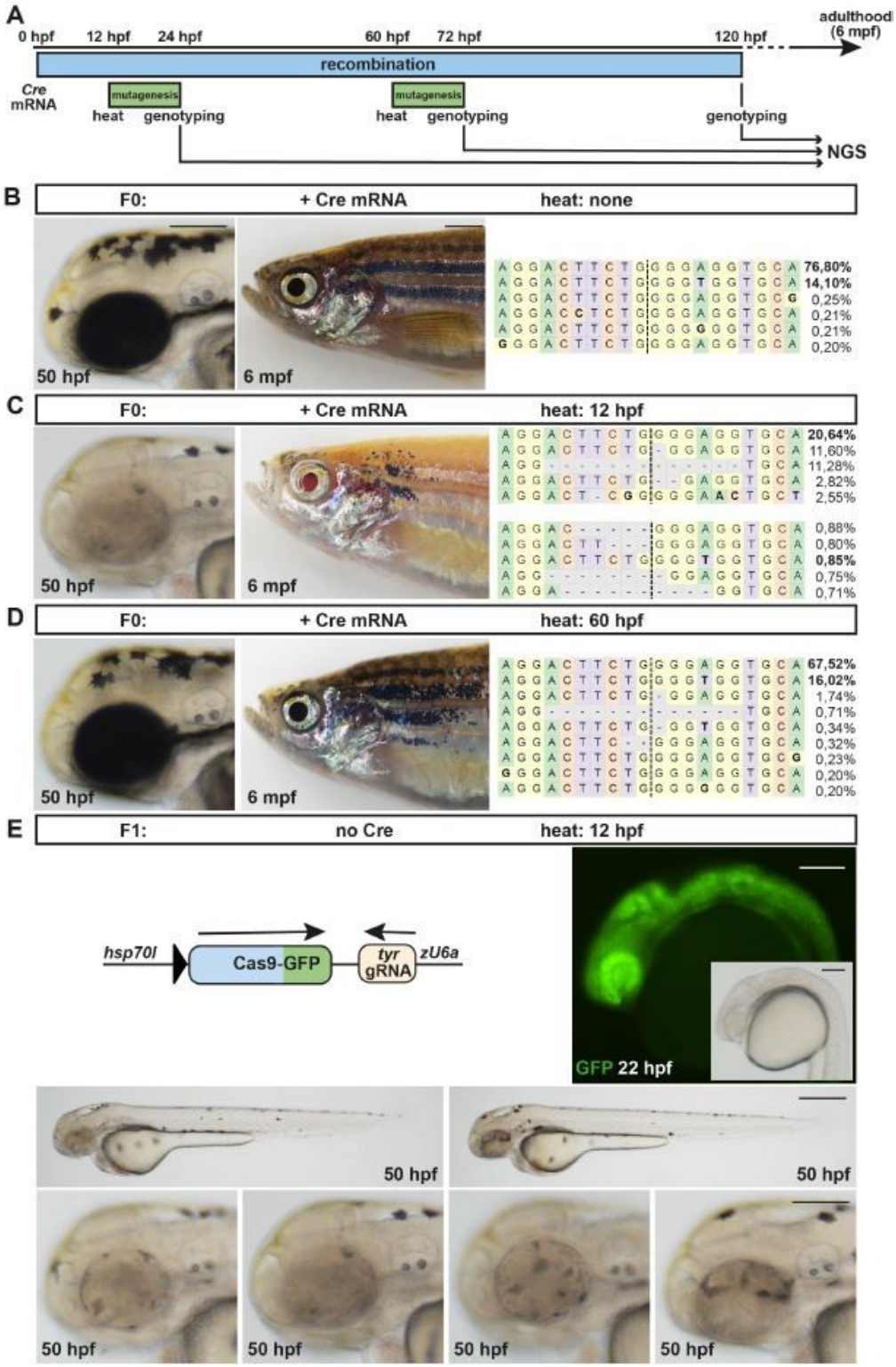

Figure 6

Temporally-controlled gene inactivation. (A) Timeline. Cre mRNA injections into progeny of 3C tyr animals at the 1-cell stage elicit ubiquitous recombination (blue box). A subset of injected embryos was heat treated at 12 or 60 hpf to trigger Cas9-GFP expression and mutagenesis of the tyr target site (green box). In addition, Cre mRNA injected animals were collected at 120 hpf without a prior heat treatment. Single embryo genotyping was applied to all specimen and ten embryos of each time point (heat: none; heat: 12

hpf; heat 60 hpf) were combined and analyzed using next generation sequencing (NGS). In addition, siblings of all three time points were raised to adulthood (6 months post fertilization (mpf)). (B) Animals subjected to Cre mRNA injection but no heat treatment show neither a pigmentation phenotype at embryonic or adult stages nor any signs of mutagenesis. (C) A strong pigmentation phenotype is observed at embryonic (50 hpf) and adult stages (6 mpf) in animals heat treated at 12 hpf. (Note almost complete absence of pigmentation in the RPE at 6 mpf making the eye appear red.) NGS confirms high level indel production. (D) Pigmentation defects are observed at adult but not at embryonic stages in animals heat treated at 60 hpf. Sequencing corroborates mutagenesis of the tyr target site. (E) The recombined 3C tyr allele is transmitted in the germline of F0 animals subjected to Cre mRNA injection only. Heat treatment in the F1 generation results in GFP expression and pigmentation defects after activation at 12 hpf. Scale bars: 500 µm for 50 hpf and 2 mm for 6 mpf in B-D; 150 µm in E, except for lower row with 500 µm.

Supplementary Files

This is a list of supplementary files associated with this preprint. Click to download.

- SupplementaryfiguresHansetal..pdf